Articel

Sequenced Combinations of Cisplatin and Selected Phytochemicals Towards Overcoming Drug Resistance in Ovarian Tumour Models

Safiah Ibrahim Althurwi, Jun Q Yu, Philip Beale, Fazlul Huq

1 University of Sydney; sssaafy2008@hotmail.com

2 University of Sydney; jun.yu@sydney.edu.au

3 Concord Repatriation General Hospital; Philip.beale@health.nsw.gov.au

4 Reman Research Sydney Australia; Fazlul.huq@bigpond.com

- Corresponding author: FH +61 411235462

Abstract

Background

In the present study, cisplatin, artemisinin and oleanolic acid were evaluated alone and in combination, on human ovarian A2780, A2780^{ZD0473R} and A2780^{cisR} cancer cell lines with aim of overcoming cisplatin resistance and side effects.

Methods

Cytotoxicity was assessed by MTT reduction assay. CI values were used as a measure of combined drug effect. MALDI TOF/TOF MS/MS and 2-DE gel electrophoresis were used to identify protein biomarkers in ovarian cancer and to evaluate combination effects.

Results

Synergism from combinations was dependent on concentration and sequence of administration. Generally, bolus was most synergistic. 49 proteins differently expressed by 2 ≥ fold were: CYPA, EIF5A1, Op18, p18, LDHB, P4HB, HSP7C, GRP94, ERp57, mortalin, IMMT, CLIC1, NM23, PSA3,1433Z, and HSP90B were down-regulated, whereas hnRNPA1, hnRNPA2/B1, EF2, GOT1, EF1A1, VIME, BIP, ATP5H, APG2, VINC, KPYM, RAN, PSA7, TPI, PGK1, ACTG and VDAC1 were up-regulated, while TCPA, TCPH, TCPB, PRDX6, EF1G, ATPA, ENOA, PRDX1, MCM7, GBLP, PSAT, Hop, EFTU, PGAM1, SERA and CAH2 were not-expressed in A2780^{cisR} cells. The proteins were found to play critical roles in cell cycle regulation, metabolism and biosynthetic processes and drug resistance and detoxification.

Conclusion

Results indicate that appropriately sequenced combinations of cisplatin with ART and OA may provide a means to reduce side effects and circumvent platinum resistance.

Keywords: Ovarian cancer, drug resistance, apoptosis, proteomics, combination, cytotoxicity, artemisinin, oleanolic acid, platinum drugs, cisplatin.

1. Introduction

Ovarian cancer is one of the major causes of death in gynecologic cancers [1] marked with absence of reliable screening methods and distinctive symptoms [2,3]. Although widely used, efficacy of platinum drugs oxaliplatin, carboplatin and cisplatin, is limited due to acquired resistance and adverse side effects. Combination treatments [4] with tumour active plant based compounds that have atypical mechanisms of action and minor or no side effects can provide a means to overcome drug resistance [5]. Resistance to platinum-based drugs [6,7] is related to four major mechanisms which are: (1) increased detoxification and degradation (such as by glutathione), (2) reduced drug accumulation (due to increased efflux and/or reduced influx), (3) increased repair of the Pt-DNA adducts, or (4) enhanced tolerance of the damaged DNA [8].

Oleanolic acid (OA) is a natural pentacyclic triterpenoid (figure 1) [9], predominantly found in olive oil [10], that exhibits antioxidant, anti-inflammatory, anticancer, and hepatoprotective activities [9]. OA is reported to inhibit metastasis, angiogenesis and invasion in different cancers [10] while it induces programmed cell death in different cancer cell lines such as osteosarcoma, liver, gastric, breast, prostate, pancreatic, colorectal, and bladder cancer cells [10] via enhancement of p38 MAPK, ASK1, ROS, and inhibition of signalling pathways such as S6K, PI3K, mTOR, Akt, and NF-kB in time and concentration dependent fashion [10]. Bit it shows pro-apoptotic and anti-proliferative effects through down-regulation of survivin, Bcl-xL, Bcl-2, and other anti-apoptosis proteins accompanied with modulation of MRP1 activity [10]. **Artemisinin (ART),** is obtained from (Sweet wormwood, *Artemisia annua* L), (figure 1) [11]. It inhibits metastasis, invasion, and

angiogenesis while it induces apoptosis and cell cycle arrest [11]. Artemisinin and its derivatives also exhibit anti-malarial, and anti-inflammatory activities [11] through modulation of molecular pathways such as tyrosine kinases, STAT-1/3/5, NF-κB, MAPKs, PI3K/Akt Sp1, Toll-like receptors, Nrf2/ ARE phospholipase, p53, and MDM2 oncogene [11]. Another study reported that artemisinins increase E-cadherin, Bax and reduce MMPs, BCL-2, HIF-1α, VEGF, CDKs, and cyclins [12]. It has been suggested that ART induces DNA damage and apoptosis by producing free radicals that result from the reaction of its endoperoxide moiety with intracellular free iron [12]. However, the effect is influenced by cancer cell phenotype and the origin of tissue [13]. A growing body of evidence suggests that the combination treatment with plant-based anticancer agents and common cancer drugs can improve effectiveness of chemotherapeutic agents through regulation of pathways, including the ones regulated by COX-2, nuclear factor-KB, and Akt (which are also associated with drug resistance) [5]. Thus, it is thought that artemisinin and oleanolic acid would act synergistically with cisplatin by regulating various pathways and repressing different mechanisms involved in cancer initiation, metastasis, invasion, and angiogenesis.

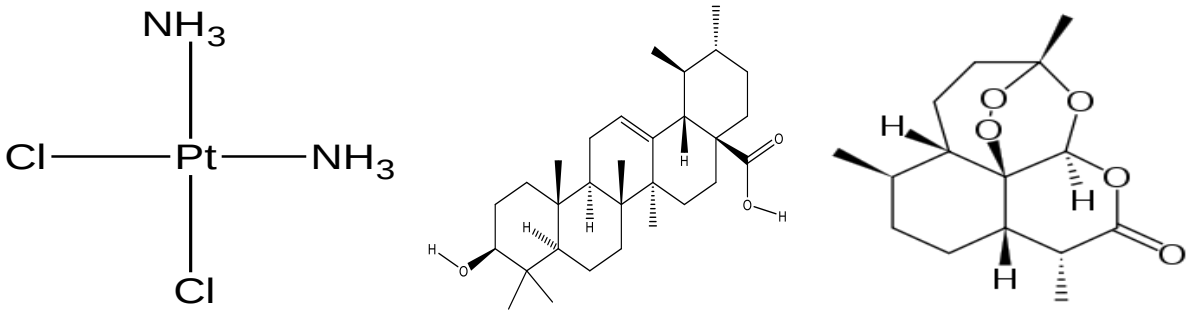

Cisplatin (CS) Oleanolic acid (OA) Artemisinin (ART)

Figure 1 Chemical structure of cisplatin, oleanolic acid and artemisinin.

The current study aimed to examine efficacy from binary combinations of artemisinin and oleanolic acid with cisplatin in A2780, A2780^{cisR} and A2780^{ZD0473R} human ovarian cancer cell lines. Selected combinations were chosen to determine their effect on cellular platinum accumulation and Pt–DNA binding levels, changes in protein expression (using 2-DE gel electrophoresis). Finally, MALDI -TOF-TOF MS/MS was used to identify the proteins.

2. Results

Results

Growth-inhibitory effect of single drugs.

The concentration of CS, OA and ART that caused 50% growth inhibition in A2780, A2780^{cisR} and A2780^{ZD0473R} cell lines, was identified as IC_{50} values. The data revealed that (table 1), the highest RF value was produced by CS, whereas the lowest was produced by OA. Among the two phytochemicals in A2780 cell line, ART was the more active, whereas, in A2780^{cisR} and A2780^{ZD0473R} cell lines, OA was the more active compound.

Table 1 IC_{50} values of CS, ART, and OA as applied to the human ovarian cancer cell lines A2780 A2780^{cisR} and A2780^{ZD0473R} cell lines based on at least triplicate measurements.

IC_{50} (μM) and *RF values					
Drug	**A2780**	**A2780^{cisR}**	***RF**	**A2780^{ZD0473R}**	***RF**
CS	0.66 ± 0.08	6.44 ± 0.11	9.75.63	8.37± 0.06	12.6
ART	16.78 ± 0 .06	26.8 ± 0.13	1.60	36.36 ± 0.09	2.16
OA	34.0 ± 0.31	26.15 ± 0.28	0.76	10.85 ± 0.05	0.3

*Resistant factors (RF)

Combination studies:

Combination indices (CIs) were calculated using the formula developed by Chou and Talalay to determine whether the combined drug action was antagonistic, synergistic or additive A CI value < 1 means a synergistic effect, equal to one means an additive effect, and > 1 means an antagonistic effect of the combined drugs [14] ED_{50}, ED_{75} and ED_{90} standing for concentrations applying respectively to 50%,75% and 90% growth inhibition, were determined for all combinations. All drugs in combination were added using the following three modes of administration: (0/0 h, 0/4 h and 4/0 h) to the selected cell lines. As regards to A2780 cell line, the data show that CS and ART (table 2 and figure 2), using 0/0 h produced the highest synergistic effect while the lowest synergistic outcome was produced from (0/4 h). In contrast, CS and OA (table 3 and figure 3), using 0/4 h showed the highest synergistic outcome and the least was produced from 4/0 h. On the other hand, in relation to $A2780^{cisR}$ cell line, CS and ART (table 3 and figure 2) using 0/0 h exhibited the highest synergistic outcome, and the lowest resulted from 4/0 h combination. Likewise, CS and OA (table 3 and figure 3) using 0/0 h produced the highest synergistic outcome, and the lowest resulted from 4/0 h combination. Moreover, regarding $A2780^{ZD473R}$ cell line, CS and ART in combination (table 4 and figure 2) using 0/0 h exhibited the highest synergistic outcome. Likewise, CS and OA in combination (table 4 and figure 3) using 0/0 h resulted in the highest synergistic outcome. The results are discussed fully in the next section.

Table 2 CI values of CS with OA and ART in A2780 cell line.

			CI Value at					
Drug	**Sequence (h)**	**Molar Ratio**	**ED_{50}**	**ED_{75}**	**ED_{90}**	***D_m**	***M**	***r**

Preprints (www.preprints.org) | NOT PEER-REVIEWED | Posted: 30 August 2020 doi:10.20944/preprints202008.0667.v1

CS			N/A	N/A	N/A	1.16	0.88	0.99
OA			N/A	N/A	N/A	37.19	0.64	1.00
CS+OA	0/0	1:51.52	0.72	0.50	0.37	0.53	1.06	0.99
CS+OA	0/4		0.68	0.59	0.54	0.49	0.86	0.97
CS+OA	4/0		0.92	1.07	1.28	0.69	0.72	0.98
ART			N/A	N/A	N/A	26.5	0.55	0.99
CS+ART	0/0	1:25.42	0.74	0.55	0.47	0.40	0.85	1.00
CS+ART	0/4		0.86	1.05	1.46	0.47	0.62	0.99
CS+ART	4/0		0.77	0.55	0.60	0.32	0.72	0.99

*Dm: medium effect dose; *m: exponent defining shape of the dose effect curve; *r: reliability coefficient

Table 3 CI values of CS with OA and ART in A2780^{cisR} cell line.

			CI Values at					
Drug	**Sequence (h)**	**Molar Ratio**	**ED_{50}**	**ED_{75}**	**ED_{90}**	***Dm**	***m**	***r**
CS			N/A	N/A	N/A	8.03	0.63	0.99
OA			N/A	N/A	N/A	56.44	0.40	1.00
CS+OA	0/0	1:4.05	0.57	0.49	0.50	2.88	0.61	1.00
CS+OA	0/4		0.63	0.42	0.32	3.15	0.72	1.00
CS+OA	4/0		0.77	0.53	0.43	3.85	0.70	0.99
ART			N/A	N/A	N/A	77.82	0.49	1.00
CS+ART	0/0	1:4.16	0.54	0.88	1.51	2.98	0.48	1.00
CS+ART	0/4		0.75	0.67	0.64	4.17	0.65	1.00
CS+ART	4/0		0.87	0.80	0.78	4.82	0.64	1.00

*Dm: medium effect dose; *m: exponent defining shape of the dose effect curve; *r: reliability coefficient.

Table 4 CI values of CS with OA and ART in ^{A2780ZD0473R} cell line.

			CI Values at					
Drug	**Sequence (h)**	**Molar Ratio**	**ED_{50}**	**ED_{75}**	**ED_{90}**	***D_m**	***m**	***r**
CS			N/A	N/A	N/A	11.35	0.83	0.98
OA			N/A	N/A	N/A	29.43	0.43	0.96
CS+OA	0/0	1:1.3	0.58	0.61	0.86	3.55	0.61	0.99
CS+OA	0/4		0.81	0.56	0.52	5.00	0.80	0.99
CS+OA	4/0		0.80	0.71	0.74	5.53	0.73	0.99
ART			N/A	N/A	N/A	17.19	0.57	0.99
CS+ART	0/0	1:4.35	0.71	0.80	0.95	1.46	0.56	1.00
CS+ART	0/4		0.82	0.91	1.36	1.71	0.53	0.99
CS+ART	4/0		0.82	0.85	1.09	1.89	0.58	1.00

*Dm: medium effect dose, *m: exponent defining shape of the dose effect curve, *r: reliability coefficient

Preprints (www.preprints.org) | NOT PEER-REVIEWED | Posted: 30 August 2020 doi:10.20944/preprints202008.0667.v1

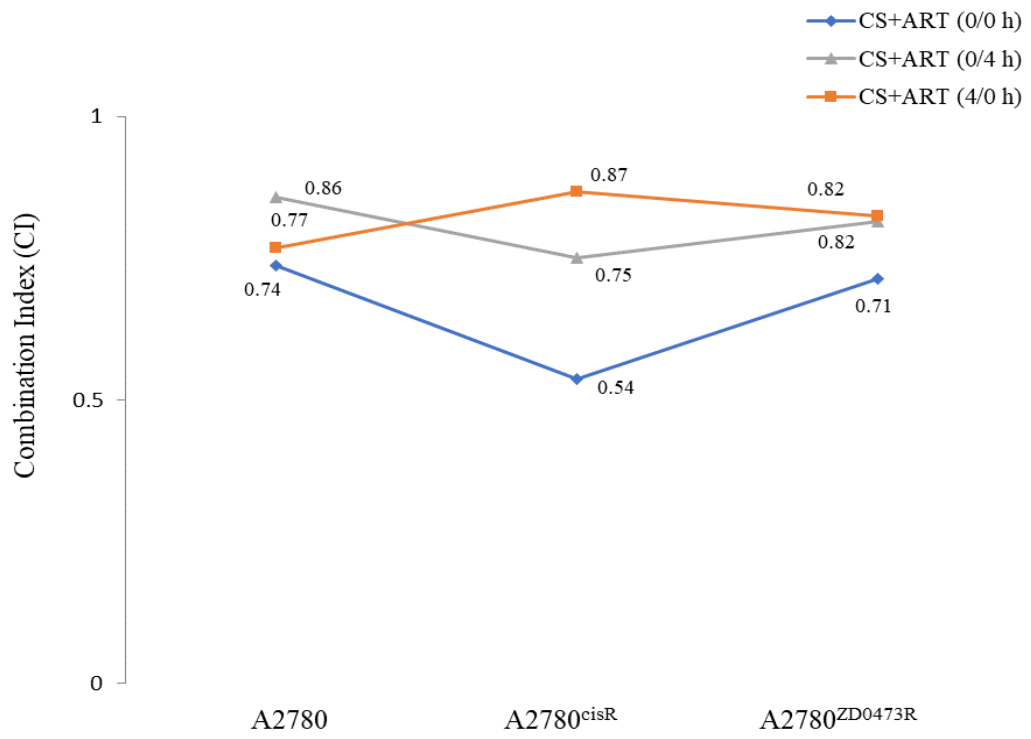

Figure 2 Graphical representation of combination indices (CI) applying to the combinations of CS with ART at ED50.

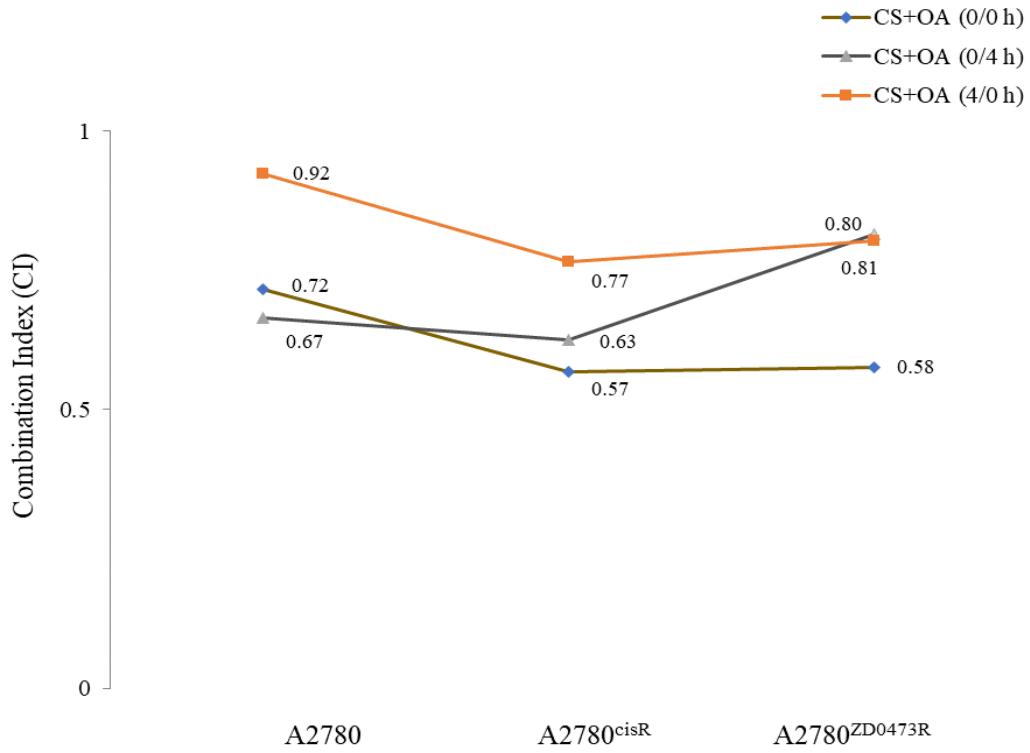

Figure 3 Graphical representation of combination indices (CI) applying to the combinations of CS with OA at ED_{50}.

Cellular accumulation of platinum and Platinum–DNA binding level

Cellular accumulation of platinum.

The data show (table 5 and figure 4) that platinum accumulations from the combinations of CS with ART or OA were always greater than those from CS alone in both the cell lines (A2780 and A2780^{cisR}), indicating that the presence of ART and OA have served either to increase the uptake or decrease the efflux or both.

Table 5 Platinum accumulation level of CS alone and in combination with ART and OA.

	*Platinum accumulation			
	A2780		A2780^{cisR}	
DRUG	Value	Fold change	Value	Fold change
CS	0.15 ± 0.01	-	0.27±0.02	-
CS+ART (0/0 h)	0.65 ± 0.04	4.33	2.29 ± 0.20	8.48
CS+ART (0/4 h)	0.91 ± 0.06	6.06	0.75 ± 0.04	2.77
CS+ART (4/0 h)	0.22 ± 0.02	1.46	1.22 ± 0.09	4.51
CS+OA (0/0 h)	2.22 ± 0.08	14.8	0.91 ± 0.08	3.33
CS+OA (0/4 h)	0.27 ± 0.01	1.8	0.50 ± 0.02	1.85
CS+OA (4/0 h)	0.22 ± 0.01	1.46	1.14 ± 0.11	4.22

*Expressed as: nmol Pt per 5x106 cells

 doi:10.20944/preprints202008.0667.v1

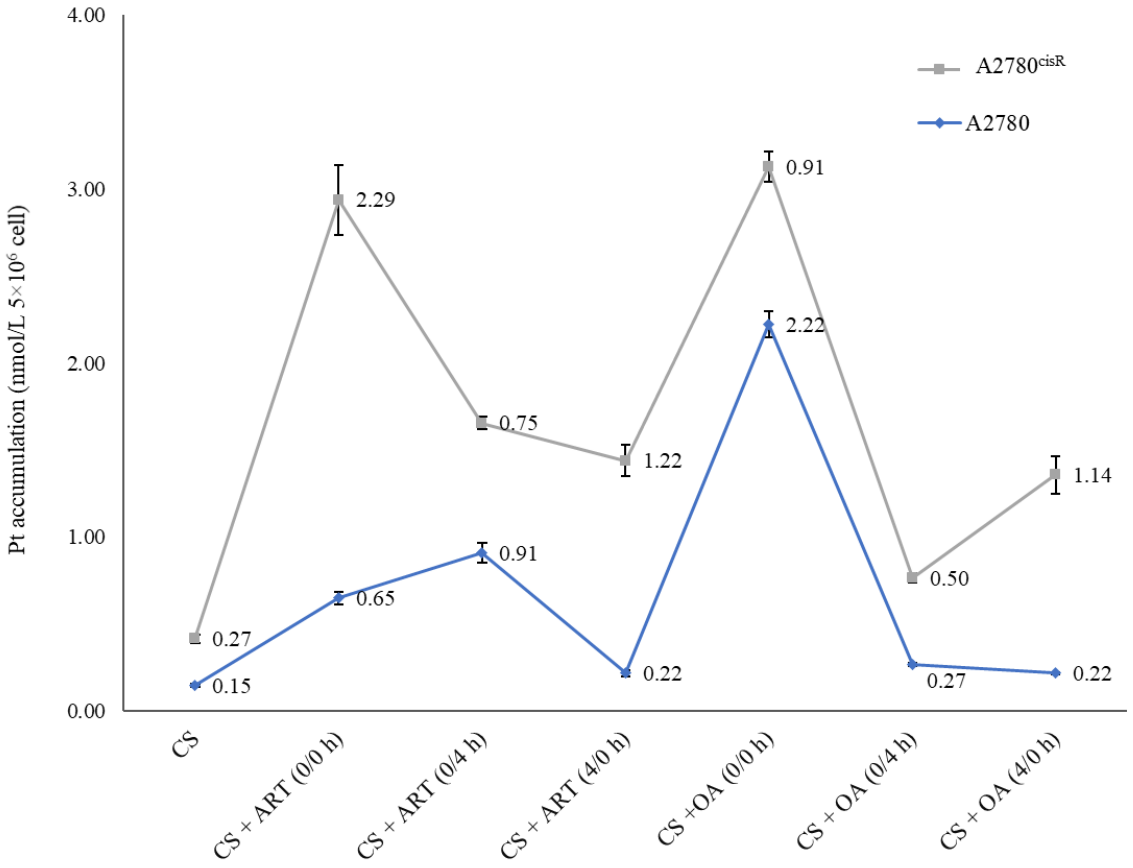

Figure 4 Platinum accumulation level from CS alone and in combination with ART and OA

Platinum-DNA binding level.

The data reveal that the platinum–DNA binding levels resulted from the combination of CS with ART or OA (table 6 and in figure 5); in A2780 were not always higher than those from CS alone, indicating that a positive correlation between increased level of CS-binding and synergistic outcomes is not always found. For example, the level of CS-DNA binding from the combination of CS with OA using 0/4 h was less than that of CS alone. Moreover, in A2780 CS-DNA binding level was a sequence-dependent but not synergistic in outcome. As the level of CS-DNA binding resulted from combinations of CS with ART using 0/0 h was lowest whereas, combination index showed that 0/0 h sequence was most synergistic sequence. On the contrary, in A2780^{ciR} cell line, platinum-DNA binding level from combination treatments was always higher than those from CS alone, suggesting

the presence of such a correlation. Moreover, the observed increase in CS-binding levels in A2780^{ciR} cell line from combination with ART and OA are consistent with the increase in CS-accumulation levels due to the treatments.

Table 6 Platinum–DNA-binding levels of CS alone and in combinations with ART and OA.

	*Platinum–DNA binding level			
	A2780		A2780^{cisR}	
DRUG	Value	Fold change	Value	Fold change
CS	6.08± 0.57	-	3.66 ± 0.49	-
CS+ ART (0/0 h)	9.24 ± 0.64	1.52	3.70 ± 0.33	1.01
CS+ ART (0/4 h)	8.26 ± 0.78	1.36	8.67 ± 0.59	2.37
CS+ ART (4/0 h)	3.22 ± 0.49	0.53	4.60 ± 0.11	1.26
CS+ OA (0/0 h)	4.13 ± 0.28	0.68	5.12 ± 0.43	1.40
CS+ OA (0/4 h)	1.66 ± 0.11	0.27	4.43 ± 0.29	1.21
CS+ OA (4/0 h)	4.71 ± 0.36	0.77	7.85 ± 0.73	2.14

*Expressed as: nmol Pt per mg of DNA

Preprints (www.preprints.org) | NOT PEER-REVIEWED | Posted: 30 August 2020 doi:10.20944/preprints202008.0667.v1

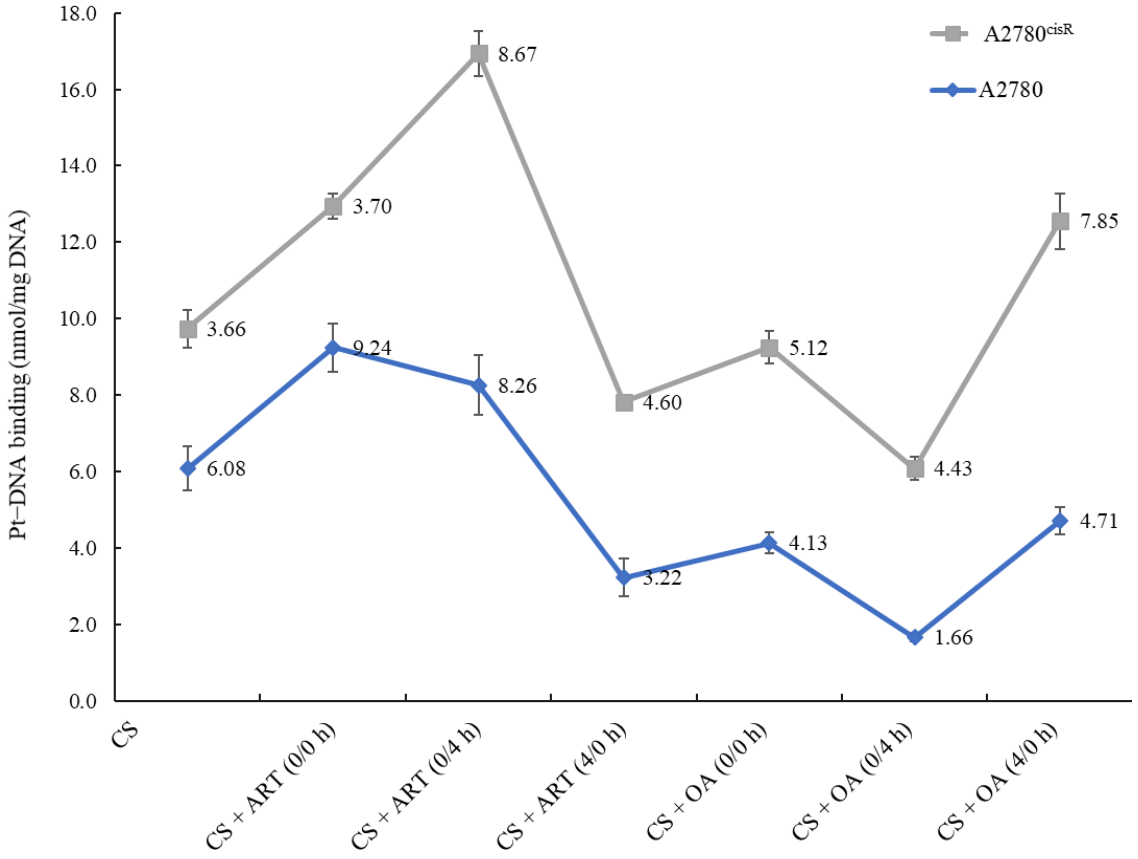

171
172
173 **Figure 5** Platinum–DNA-binding levels of CS alone and in combinations with ART and OA.
174

175 **Proteomics** has analyzed causes of drug resistance in terms of the changes in protein
176 expression and has argued that ATR and OA would be able to regulate the expression level of
177 those proteins. Thus, proteins in A2780 and A2780^{cisR} cell lines were inspected by 2D-gel
178 electrophoresis and mass spectrometry to examine their association with platinum drug
179 resistance, wherein the protein expression levels in A2780^{cisR} cell line were compared to
180 what were found in its counterpart cell line to determine the proteins that were differentially
181 expressed. The objective of the proteomic study, besides the determination of new ovarian
182 cancer biomarkers, was to evaluate the effect of (CS and ART using 0/0 h), (CS and OA
183 using 0/4 h), (CS and ART using 0/0 h) and (CS and OA using 0/0 h) on the expression of

184 those dysregulated proteins (differently expressed proteins). Tables 7-8 show proteins
185 expression in: 1) untreated A2780^{cisR} as compared to the values found in untreated A2780
186 cell line, and 2) treated A2780^{cisR} cell line (with the chosen drug treatments as mentioned
187 above) as compared to the values that were detected in both untreated cell lines. In both
188 situations, at the beginning A2780 cell line was used as a reference. Later A2780^{cisR} cell line
189 was used as the reference. Proteins were considered to have undergone significant changes in
190 expression if the fold factor was ≥ 2.0 (tables 7-9). The proteins that were detected by
191 MALDI TOF/TOF MS and were matched against Mascot database
192 (http://www.matrixscience.com) and UniProtKB / Swiss Prot database
193 (http://www.uniprot.org/) [15], when A2780 and A2780^{cisR} cell lines alternatively were used
194 as a reference, are illustrated in tables 9-10. Accession number, protein ID, name and mass,
195 MSMS, degree of coverage and score were obtained from APAF
196 (http://www.proteome.org.au/). Theoretical isoelectric point (*pI*) , subcellular location, mass
197 spectrum, and matched peptides were obtained from Mascot database
198 (http://www.matrixscience.com) and SwissProt database (http://www.uniprot.org/) [15] through
199 APAF (http://www.proteome.org.au/). In this study, 49 proteins out of 101 scored above 56,
200 according to Mascot parameter that protein scores above 56 is considered significant (see,
201 Mascot database (http://www.matrixscience.com), SwissProt database
202 (http://www.uniprot.org/) [15], and APAF (http://www.proteome.org.au/). Accordingly, those
203 proteins were investigated for their involvement in the development of platinum resistance,
204 besides evaluating the effect of the selected drug treatments on their expression.

205

206 **Table 7** List of protein expressions in A2780, compared to A2780^{cisR} using A2780 as reference

207

Match ID	Expression in A2780^{cisR} / A2780	CS+ART (4/0 h)	CS+OA (0/4 h)	CS+ART (0/0 h)	CS+OA (0/0 h)	Match ID	Expression in A2780^{cisR} / A2780	CS+ART (4/0 h)	CS+OA (0/4 h)	CS+ART (0/0 h)	CS+OA (0/0 h)
1	UR			PR	FUR	**48**	ND		OR		
3	DR	PR	PR	PR		**51**	DR	OR	PR	PR	PR
4	DR			PR	PR	**52**	ND	PR	PR	OR	
5	DR	PR	PR	PR		**54**	DR	OR	OR	OR	OR
7	DR			OR		**55**	DR			PR	PR
8	ND	PR	PR	OR	OR	**62**	DR				
11	ND	OR		PR		**63**	DR			PR	
12	ND	PR		PR		**66**	ND				
13	DR		PR	OR	OR	**68**	UR				
14	NC			OR	OR	**69**	DR			OR	OR
15	UR			OR	OR	**70**	ND			OR	
16	UR	PR		PR	PR	**74**	ND		OR	OR	
17	ND	OR	PR	OR	OR	**76**	UR				
19	DR	OR	PR	OR	OR	**78**	ND				
20	ND			OR	OR	**82**	ND				
21	UR				FUR	**85**	ND				
25	ND			OR	PR	**88**	ND				
27	ND	PR	OR	PR		**89**	ND			FR	OR
29	ND	OR				**94**	ND	OR	OR	OR	OR
31	ND		PR	OR		**95**	ND	OR			OR
32	ND		PR	OR	FR	**96**	ND			OR	OR
33	ND		PR	OR		**97**	ND	OR	OR		
34	ND		OR	OR		**98**	ND				
35	DR			PR	OR	**102**	ND				
36	UR		OR	OR	PR	**103**	DR		OR		
39	ND					**105**	ND				
40	DR					**106**	ND			OR	
42	ND		OR	OR		**108**	ND				
43	ND					**111**	ND		OR		
44	ND		OR			**116**	UR		PR		PR
45	DR	PR	FDR	FDR	FDR	**119**	ND			OR	
46	DR					**120**	ND		OR		

 doi:10.20944/preprints202008.0667.v1

Match ID	Expression in A2780^{cisR} / A2780	CS+ART (4/0 h)	CS+OA (0/4 h)	CS+ART (0/0 h)	CS+OA (0/0 h)	Match ID	Expression in A2780^{cisR} / A2780	CS+ART (4/0 h)	CS+OA (0/4 h)	CS+ART (0/0 h)	CS+OA (0/0 h)
47	UR	OR	OR	OR	OR	**122**	ND				

FR: Fully restored (The expression level of the protein after treatment was the same as its expression level in the untreated A2780 cell line).

OR: Over restored (means the value of protein's expression after treatment is ± 0.05, as compared to its level in the untreated A2780 cell line); FDR: Further down-regulated (the combined treatment had a negative effect on protein expression where the expression decreased at least 0.05, below the expression level compared to its level in the untreated A2780^{cisR} cell line).;FUR: Further up-regulated (the combined treatment has negatively affected the protein expression where the expression increased at least 0.05, above the expression level compared to its level in the untreated A2780^{cisR} cell line); PR: Partially-restored; UP: Up-regulated; DR: Down-regulated Blank: spot was not detected after treatment with selected combination.

Table 8 List of protein expressions in, A2780^{cisR} compered to A2780 using A2780^{cisR} as reference

Match ID	Expression in A2780^{cisR} / A2780	CS+ART (4/0 h)	CS+OA (0/4h)	CS+ART (0/0 h)	CS+OA (0/0 h)
8	UR				
9	UR	OR	PR	PR	
11	DR	OR		OR	OR
12	UR		PR	OR	PR
13	UR	PR		OR	FR
16	ND				
18	ND	OR		PR	
19	DR		OR	OR	OR
22	UR	PR	PR	PR	FUR
25	UR			PR	
26	UR		FUR		FUR
28	DR	OR		OR	
29	ND			FUR	FUR
30	UR		OR	OR	PR
32	UR	FUR	PR	FUR	FUR
41	UR			PR	PR
44	DR			PR	OR
46	UR			PR	PR
47	UR			OR	
50	UR				
56	UR				
57	UR				
58	UR			PR	PR
59	DR				
61	UR		PR		
62	UR		FUR		
63	UR	PR	PR		
69	DR			OR	

FR: Fully restored (The expression level of the protein after treatment was the same as its expression level in the untreated A2780 cell line); OR: Over restored (means the value of protein's expression after treatment is ± 0.05, as compared to its level in the untreated A2780 cell line); FDR: Further down-regulated (the combined treatment had a negative effect on protein expression where the expression decreased at least 0.05, below the expression level compared to its level in the untreated A2780^{cisR} cell line); FUR: Further up-regulated (the combined treatment has negatively affected the protein expression where the expression increased at least 0.05, above the expression level compared to its level in the untreated A2780^{cisR} cell line); Blank: spot was not detected after treatment with selected combination; PR: Partially-restored; UP: Up-regulated; DR: Down-regulated.

225
226
227 **Table 9** Characteristics of proteins that have undergone differential expressions in A2780 and A2780^{cisR} cell lines
228 following treatment with selected drug combinations using A2780 cell line as reference.
229

Mach ID	Protein ID	Full name	Mascot search results	Location	References
3	CYPA P62937	Cyclophilin A	Mass: 18001 Mascot score: 252 Coverage: 53% *pI:* 7.68 MS:15 MSMS:3	Cytoplasm	[15] http://www.matrixscience.com
4	EIF5A1 P63241	Eukaryotic initiation factor 5A isoform 1	Mass: 16821 Mascot score:168 Coverage: 51% *pI*:5.08 MS:7 MSMS:2	Cytoplasm Nucleus. Endoplasmic reticulum membrane	[15] http://www.matrixscience.com
5	p18 P23528	18 kDa phosphoprotein	Mass: 18491 Mascot score: 137 Coverage: 42% *pI*: 8.22 MS:14 MSMS:2	Nucleus matrix. Cytoplasm, cytoskeleton. cell projection	[15] http://www.matrixscience.com
7	Op18 P16949	Oncoprotein 18	Mass: 17292 Mascot score: 114 Coverage: 53% *pI*: 5.76 MS:11 MSMS:2	Cytoplasm, cytoskeleton	[15] http://www.matrixscience.com
8	PRDX1 Q06830	Peroxiredoxin-1	Mass: 22096 Mascot score: 400 Coverage: 59% *pI*: 8.27 MS:20 MSMS:6	Cytoplasm	[15] http://www.matrixscience.com
11	PGAM1 P18669	Phosphoglycerate mutase 1	Mass: 28786 Mascot score: 318 Coverage: 64% *pI*: 6.67		[15] http://www.matrixscience.com

 doi:10.20944/preprints202008.0667.v1

Mach ID	Protein ID	Full name	Mascot search results	Location	References
			MS:17 MSMS:3		
13	1433Z P63104	14-3-3 protein zeta/delta	Mass: 27728 Mascot score: 216 Coverage: 61% *pI*: 4.73 MS:22 MSMS:4	Cytoplasm	[15] http://www.matrixscience.com
15	hnRNPA1 P09651	Heterogeneous nuclear ribonucleoprotein A1	Mass: 38723 Mascot score: 325 Coverage: 46% *pI*: 9.17 MS:22 MSMS:5	Nucleus. Cytoplasm	[15] http://www.matrixscience.com
16	hnRNPA2/B1 P22626	Heterogeneous nuclear ribonucleoproteins A2/B1	Mass: 37407 Mascot score: 267 Coverage: 49% *pI*: 8.97 MS:19 MSMS:4	Nucleus, nucleoplasm. Cytoplasm	[15] http://www.matrixscience.com
17	ENOA	Alpha-enolase	Mass: 37407 Mascot score: 331 Coverage 44% *pI*: 7.01 MS:23 MSMS:5	Cytoplasm. Cell membrane.	[15] http://www.matrixscience.com
19	LDHB P07195	L-lactate dehydrogenase B chain;	Mass: 36615 Mascot score: 81 Coverage: 46% *pI*: 5.71 MS:24 MSMS:6	Cytoplasm	[15] http://www.matrixscience.com
25	EFTU P49411	Elongation factor Tu, mitochondrial	Mass: 49510 Mascot score: 499 Coverage: 49% *pI*: 7.26 MS:22 MSMS:7	Mitochondrion	[15] http://www.matrixscience.com

Mach ID	Protein ID	Full name	Mascot search results	Location	References
27	EF1G P26641	Elongation factor 1-gamma	Mass: 50087 Mascot score: 389 Coverage: 42% *pI: 6.25* MS:23 MSMS:5		[15] http://www.matrixscience.com
31	ENOA P06733	Alpha-enolase	Mass: 47139 Mascot score: 331 Coverage: 44% *pI*: 7.01 MS:23 MSMS:5	Cytoplasm. Cell membrane	[15] http://www.matrixscience.com
32	TCPB P78371	T-complex protein 1 subunit beta	Mass: 57452 Mascot score: 91 Coverage: 39% *pI*: 6.01 MS: 30 MSMS: 0	Cytoplasm	[15] http://www.matrixscience.com
33	SERA O43175	D-3-phosphoglycerate dehydrogenase	Mass: 56614 Mascot score: 213 Coverage: 25% *pI*: 6.29 MS: 15 MSMS: 4	Cytosol	[15] http://www.matrixscience.com
35	ERp57 P30101	Endoplasmic reticulum resident protein 57	Mass: 56747 Mascot score: 521 Coverage: 48% *pI*: 5.98 MS: 6 MSMS: 31	Endoplasmic reticulum	[15] http://www.matrixscience.com
36	VIME P08670	Vimentin	Mass: 53619 Mascot score: 609 Coverage: 75% *pI*: 5.06 MS: 51 MSMS: 4	Cytoplasm	[15] http://www.matrixscience.com
39	TCPH Q99832	T-complex protein 1 subunit eta	Mass: 59329 Mascot score: 84 Coverage: 25% *pI: 7.55*	Cytoplasm	[15] http://www.matrixscience.com

 doi:10.20944/preprints202008.0667.v1

Mach ID	Protein ID	Full name	Mascot search results	Location	References
			MS: 19 MSMS: 2		
45	HSP7C P11142	Heat shock cognate 71 kDa protein	Mass: 70854 Mascot score: 705 Coverage: 62% *pI: 5.37* MS: 45 MSMS: 6	Cytoplasm	[15] http://www.matrixscience.com
46	Mortalin P38646	Stress-70 protein	Mass: 73635 Mascot score: 189 Coverage: 17% *pI: 5.87* MS: 10 MSMS: 5	Mitochondrion	[15] http://www.matrixscience.com
47	BIP P11021	Immunoglobulin heavy chain-binding	Mass: 72288 Mascot score: 345 Coverage: 46% *pI: 5.07* MS: 33 MSMS:6	Endoplasmic reticulum lumen	[15] http://www.matrixscience.com
51	HSP90B P08238	Heat shock protein HSP 90-beta	Mass: 83212 Mascot score: 623 Coverage: 40% *pI: 4.97* MS: 37 MSMS:7		[15] http://www.matrixscience.com
52	EF2 P13639	Elongation factor 2	Mass: 95277 Mascot score: 431 Coverage: 32% *pI*: 6.41 MS: 47 MSMS:7		[15] http://www.matrixscience.com
54	GRP94 P14625	94 kDa glucose-regulated protein	Mass: 92411 Mascot score: 99 Coverage: 22% *pI: 4.76* MS: 18 MSMS:2	Endoplasmic reticulum lumen	[15] http://www.matrixscience.com

 doi:10.20944/preprints202008.0667.v1

Mach ID	Protein ID	Full name	Mascot search results	Location	References
55	IMMT Q16891	Mitochondrial inner membrane protein	Mass: 83626 Mascot score: 136 Coverage: 29% *pI: 6.08* MS: 23 MSMS:1	Mitochondrion inner membrane	[15] http://www.matrixscience.com
63	NM23 P15531	Metastasis inhibition factor nm23	Mass: 17138 Mascot score: 405 Coverage: 60% *pI*: 5.83 MS: 12 MSMS:6	Cytoplasm	[15] http://www.matrixscience.com
66	PRDX6 P30041	Peroxiredoxin-6	Mass: 25019 Mascot score: 342 Coverage: 51% *pI*: 6.00 MS: 15 MSMS:5	Cytoplasm	[15] http://www.matrixscience.com
69	PSA3 P25788	Proteasome subunit alpha type-3	Mass: 28415 Mascot score: 125 Coverage: 50% *pI: 5.19* MS: 15 MSMS: 3	Cytoplasm	[15] http://www.matrixscience.com
76	hnRNPA2/B1 P22626	Heterogeneous nuclear ribonucleoproteins A2/B1	Mass: 37407 Mascot score: 220 Coverage: 55% *pI*: 8.97 MS: 20 MSMS: 2	Nucleus, nucleoplasm	[15] http://www.matrixscience.com
88	Hop P31948	Hsc70/Hsp90-organizing protein	Mass: 62599 Mascot score: 375 Coverage: 52% *pI: 6.40* MS: 45 MSMS: 6	Cytoplasm (By similarity).	[15] http://www.matrixscience.com
89	MCM7 P33993	DNA replication licensing factor MCM7	Mass: 81257 Mascot score: 214 Coverage: 54% *pI*: 6.08	Nucleus (By similarity)	[15] http://www.matrixscience.com

 doi:10.20944/preprints202008.0667.v1

Mach ID	Protein ID	Full name	Mascot search results	Location	References
			MS: 40 MSMS:3		
94	GBLP P63244	Guanine nucleotide-binding protein subunit beta-2-like 1	Mass: 35055 Mascot score: 189 Coverage: 37% *PI: 7.60* MS: 16 MSMS:2	Cell membrane; Peripheral membrane protein.	[15] http://www.matrixscience.com
95	PSAT Q9Y617	Phosphohydroxythreonine aminotransferase	Mass: 40397 Mascot score: 437 Coverage: 41% *pI: 7.56* MS: 21 MSMS:7	(UniPortKB 2014) (http://www.matrixscience.com)	[15] http://www.matrixscience.com
96	VIME P08670	Vimentin	Mass: 53619 Mascot score: 452 Coverage: 71% *pI*: 5.06 MS: 48 MSMS:7	Cytoplasm.	[15] http://www.matrixscience.com
97	ATPA P25705	ATP synthase subunit alpha, mitochondrial	Mass: 59714 Mascot score: 363 Coverage: 56% *pI: 9.16* MS: 32 MSMS:5	Mitochondrion inner membrane	[15] http://www.matrixscience.com
102	RUVB1 Q9Y265	RuvB-like 1	Mass: 50196 Mascot score: 106 Coverage: 24% *pI: 6.02* MS: 17 MSMS:4	Nucleus matrix	[15] http://www.matrixscience.com
105	TCPA P17987	T-complex protein 1 subunit alpha	Mass: 60306 Mascot score: 167 Coverage: 43% *pI: 5.80* MS: 21 MSMS:3	Cytoplasm	[15] http://www.matrixscience.com

Mach ID	Protein ID	Full name	Mascot search results	Location	References
108	CAH2 P00918	Carbonic anhydrase 2	Mass: 29228 Mascot score: 159 Coverage: 27% *pI: 6.87* MS: 7 MSMS:3	Cytoplasm	[15] http://www.matrixscience.com
116	PRS7 P35998	26S protease regulatory subunit 7	Mass: 48603 Mascot score: 98 Coverage: 45% *pI: 5.71* MS: 20 MSMS: 1	Cytoplasm	[15] http://www.matrixscience.com

* Accession number, protein ID, names and Mass, MSMS, coverage and protein score were obtained from APAF (http://www.proteome.org.au/); *Theoretical isoelectric point (pI), subcellular location mass spectrum and matched peptides were obtained from Mascot database (http://www.matrixscience.com), SwissProt database), (http://www.uniprot.org/) [15]; *Protein scores from Mascot database (http://www.matrixscience.com) through APAF (http://www.proteome.org.au/).

234

235 **Table 10** Characteristics of proteins that have undergone differential expressions in A2780 and A2780^{cisR} cell lines
236 following treatment with selected drug combinations using A2780^{cisR} cell line as reference.
237

Mach ID	Protein ID	Full name	Mascot search results	Location	References
8	ATP5H O75947	ATP synthase subunit d, mitochondrial	Mass: 18480 Mascot score: 128 Coverage: 57% *pI: 5.21* MS: 11 MSMS: 3	Mitochondrion	[15] http://www.matrixscience.com
9	RAN P62826	GTP-binding nuclear protein Ran	Mass: 24408 Mascot score: 132 Coverage: 39% *pI: 7.01* MS: 11 MSMS:1	Nucleus	[15] http://www.matrixscience.com
12	PSA7 O14818	Proteasome subunit alpha type-7	Mass: 27870 Mascot score: 85 Coverage: 39% *pI*: 8.60 MS: 10 MSMS: 1	Cytoplasm.	[15] http://www.matrixscience.com
13	TPI P60174	Triosephosphate isomerase	Mass: 30772 Mascot score: 340 Coverage: 49% *pI*: 5.65 MS: 20 MSMS:3		[15] http://www.matrixscience.com
16	VDAC1 P21796	Voltage-dependent anion-selective channel protein 1	Mass: 30754 Mascot score: 368 Coverage: 51% *pI: 8.62* MS: 12 MSMS: 3	Mitochondrion outer membrane	[15] http://www.matrixscience.com
18	hnRNPA2/B1 P22626	Heterogeneous nuclear ribonucleoproteins A2/B1	Mass: 37407 Mascot score: 258 Coverage: 48% *pI: 8.97* MS: 21 MSMS: 6	Nucleus, nucleoplasm	[15] http://www.matrixscience.com

 doi:10.20944/preprints202008.0667.v1

Mach ID	Protein ID	Full name	Mascot search results	Location	References
22	PGK1 P00558	Phosphoglycerate kinase 1	Mass: 44586 Mascot score: 145 Coverage: 48% *pI: 8.30* MS: 22 MSMS: 1	Cytoplasm.	[15] http://www.matrixscience.com
25	GOT1 P17174	Glutamate oxaloacetate transaminase 1	Mass: 46219 Mascot score: 331 Coverage: 66% *pI: 6.52* MS: 27 MSMS: 6	Cytoplasm	[15] http://www.matrixscience.com
30	EF1A1 P68104	Elongation factor 1-alpha 1	Mass: 50109 Mascot score: 135 Coverage: 25% *PI: 9.10* MS: 13 MSMS: 2	Cytoplasm	[15] http://www.matrixscience.com
32	ACTG P63261	Actin, cytoplasmic 2	Mass: 41766 Mascot score: 598 Coverage: 55% *pI: 5.31* MS:26 MSMS:5	Cytoplasm, cytoskeleton	[15] http://www.matrixscience.com
41	KPYM P14618	Pyruvate kinase PKM	Mass: 57900 Mascot score: 188 Coverage: 33% *pI: 7.96* MS: 23 MSMS: 3	Cytoplasm.	[15] http://www.matrixscience.com
44	P4HB P07237	Prolyl 4-hydroxylase subunit beta	Mass: 57081 Mascot score: 433 Coverage: 50% *PI*: 4.76 MS: 29 MSMS: 6	Endoplasmic reticulum lumen	[15] http://www.matrixscience.com
57	APG2 P34932	Shock 70-related protein APG-2	Mass: 94271 Mascot score: 125 Coverage: 25% *pI*: 5.11 MS: 22	Cytoplasm (Probable)	[15] http://www.matrixscience.com

Mach ID	Protein ID	Full name	Mascot search results	Location	References
			MSMS:3		
58	VINC P18206	Vinculin	Mass: 123722 Mascot score: 226 Coverage: 34% *pI: 5.50* MS: 40 MSMS:4	Cytoplasm, cytoskeleton	[15] http://www.matrixscience.com
63	EF2 P13639	Elongation factor 2	Mass: 95277 Mascot score: 425 Coverage: 27% *pI: 6.41* MS: 39 MSMS:7	Cytoplasm	[15] http://www.matrixscience.com
69	CLIC1 O00299	Chloride intracellular channel protein 1	Mass: 26906 Mascot score: 158 Coverage: 47% *pI: 5.09* MS: 11 MSMS: 3	Nucleus	[15] http://www.matrixscience.com

* Accession number, protein ID, names and Mass, MSMS, coverage and protein score were obtained from APAF (http://www.proteome.org.au/)

*Theoretical isoelectric point (*pI*), subcellular location mass spectrum and matched peptides were obtained from Mascot database (http://www.matrixscience.com), SwissProt database (http://www.uniprot.org/) [15].

*Protein scores from Mascot database (http://www.matrixscience.com) through APAF (http://www.proteome.org.au/).

4. Discussion

4.1Cytotoxicity of single drug.

The results show that OA showed greater activity against $A2780^{cisR}$ and $A2780^{ZD0473R}$ cell lines than against parent A2780 cell line, ART showed greater sensitivity towards A2780 and $A2780^{cisR}$ than $A2780^{ZD0473R}$ cells while CS showed lower activities towards $A2780^{cisR}$ and $A2780^{ZD0473R}$ cell lines than the parent cell line. It has been reported that most of the natural products can modify several factors involved in the oncogenic transcription such as; Nrf-2, Hh /GLI, STAT3, FoxM1, PPAR y, Wnt/ β-catenin, HGFR, HIF1 α, AP-1 and NF-kB [16]. In contrast, aberrant expression of STAT3, HIF1 α, NF-kB, AP-1 and FoxM1 are often observed in different type of cancers [16]. That OA was found to be more active against $A2780^{cisR}$ and $A2780^{ZD0473R}$ cell lines may be attributed to its apoptotic effect, including the enhancement of p38 MAPK, ASK1 and ROS, and its inhibition effect of signalling pathways such as; S6K, PI3K, mTOR, Akt and NF-kB [10]. These functions make the OA more active towards platinum resistant cells.

4.2 Combination indices

The results show that the synergistic (figure 2-3 and table 2 to 4) effect from the combinations of CS with OA and ART were dependent on the dose and the sequence of administration in the three cell lines. The synergism from combination of OA and ART with CS however, is not surprising given the fact that OA and ART are known as apoptotic inducers (through increasing Bax, decreasing Bcl-2 and up-regulating of caspases), as well as they exhibit tumour inhibition effect (through the down-regulation of NF-κB and other signaling pathways) and anti-angiogenic effect (through the decreasing of VEGF) [10,17]. Hence, growth inhibition resulting from combination of OA and ART with CS may be attributed to the down-regulation of Bcl-2 and NF-κB pathways. Additionally, synergistic outcomes can be ascribed to the effect of ART on cell-cycle that involves suppression of CDK4 and CDK2 expressions [13] as well as inhibition of cyclin A, cyclin E, cyclin D3, cyclin D1, CDK6, E2F1 and JAB1 transcriptions with enhancement of IFIT3, p21, and p27 [17]. Furthermore, it is likely that the significant increase in

growth inhibition may be partly attributed to OA's anticancer effect through the regulation of various signaling cascades, including the inhibition of S6K, PI3K, mTOR, Akt and NF-kB signaling pathways [10]. The reason why 0/0 h sequence of administration of CS in combinations with ART and OA have generally produced the most synergistic outcomes, may be attributed to the time-dependent nature of the actions of ART and OA. In addition, Ziberna et al. reported that, in different multi-drug resistant cancer cell lines, OA exerts its apoptotic effect via the enhancement of p38 MAPK, ASK1and ROS pathways in time and concentration-dependent fashion [10]. Similar to our results enhanced growth inhibition in HCC was observed from co-administration of OA and sorafenib (chemotherapeutic drug) [10]. It is possible that presence of ART or OA might influence platinum influx and efflux, apoptosis induction, Pt DNA adducts tolerance, and DNA repair. In support of the idea, it may be noted that Ziberna et al. suggested that intracellular concentration levels of chemotherapeutic drugs were enhanced because of OA's ability to inhibit the efflux transporters [10]. The combination of OA with 5-fluorouracil also produced synergistic effect and induced apoptosis in pancreatic cancer. Thus, it was suggested that the combining of OA with other chemotherapeutic drugs would produce synergistic anticancer effect [10].

4.3 Cellular accumulation of platinum

The results showed that Pt accumulations (table 5 and figure 4) from combination of CS with the chosen drugs were always greater than that from CS alone, irrespective of nature of the combined drug action. For example, CS in combination with ART and OA using 0/0 h have produced greater Pt accumulations than those from the other sequences in the A2780 cell line. The Pt level from synergistic combination of CS with ART using 0/0 h was 2.9 times higher than the levels from the treatment with (4/0 h) combination of the compounds in the same cell line. Additionally, Pt level from the synergistic combination of CS and ART using 0/4 h, in A2780 cells, was about 4 times greater from the synergistic 4/0 h combination in the same cell line. Moreover, platinum level resulting from the synergistic 0/0 h combination of CS with ART

 doi:10.20944/preprints202008.0667.v1

showed 3 times higher value than that from 0/4 h combination in A2780^{cisR} cells and 8.5 times higher than that from CS alone. Furthermore, in A2780^{cisR} cells, Pt level resulted from the synergistic 4/0 h combination of CS and ART was nearly 2 times greater than that from synergistic 0/4 h combination and 4.5 times greater than that from CS alone. Together, these findings provide further support for the hypothesis that the ART growth inhibition action is a sequence and cell type dependent. The results are in agreement with the findings of Gong et al. wherein they reported that ART action was a cell type dependent [13]. On the other hand, synergistic combination of CS with OA using 0/0 h combination in A2780 cells, has increased Pt level to around 15 times greater than that from CS alone, 8.2 and 10 times greater than that from the synergistic sequences of 0/4 h and 4/0 h respectively. Furthermore, it was found that in A2780^{cisR} cell line, Pt level from synergistic combination of CS with OA using 0/0 h sequence was nearly 2 times greater than that from treatment with 0/4 h combination and 3.3 times greater than that from CS alone. Also, treatment with synergistic combination 4/0 h, CS accumulation was 1.3 times greater than that resulted from 0/0 h combination and 4 times greater than that from CS alone. It appears that intracellular accumulation of CS in the presence of OA is also sequence-dependent. Thus, the observed increase in CS accumulation could be attributed to either the ability of OA to increase the influx of CS or to decrease CS efflux or both. The findings are supported by those of Ziberna et al. wherein they reported that intracellular concentration levels of chemotherapeutic drugs were enhanced because of OA's ability to inhibit the efflux transporters [10]. The inconsistency may be due to the fact that actions of OA are time and concentration dependent [10].

4.4 Platinum-DNA binding level

Generally, platinum-DNA levels were greater in the A2780^{cisR} cells than in A278 cells. A possible explanation is that the presence of ART and OA might have modulated some of the platinum resistance mechanisms, such as decreases in platinum-DNA adducts formation [18], increased platinum detoxification, and increased DNA repair [19]. Another possible

 doi:10.20944/preprints202008.0667.v1

explanation is that the compounds led to an increase in the platinum uptake so that more platinum was available to bind DNA. Additionally, the compounds could have prevented efflux of the platinum so that the platinum had more chance to cause DNA damages before being deactivated. Combination of CS with ART and OA increased Pt-DNA binding levels, which are consistent with the observed increase in Pt accumulation resulting from the combination of CS with the phytochemicals. Overall, the results presented in (Table 6 and Figure 5) showed that with the combinations of CS with ART and OA in A2780 cell line, platinum-DNA binding levels were not always higher than those of CS alone. For example, in A2780 cell line, platinum-DNA binding levels from synergistic combination of CS with OA using 0/4 h sequence and synergistic combination of CS with ART using 4/0h sequence were significantly lower than that from CS alone. These results have highlighted the complexity of the situation due to involvement of multiple pathways associated with apoptosis and drug resistance, including the interaction between ART and OA with CS. t can thus be suggested that the variations in the overall outcomes, could be attributed to:1) the dual behavior of most of the phytochemicals as antioxidant agent (protective effect) at low concentrations and as a prooxidant (apoptotic) enhancement at high concentrations, 2) concentration and time dependent effect of the phytochemicals, 3) growth inhibitory effect of platinum drugs as stated previously not being merely dependent on abilities to bind to DNA, (although it is an essential step but not sufficient for the apoptosis induction), 4) ROS formed by platinum drugs, for example cisplatin, is dependent on its concentration and the duration of exposure [18] thereby enhancing apoptosis induction [18]. For instance, in this study 24 hours incubation period was used as against 72 hours for studies on cytotoxicity that may contribute to the overall outcomes. Finally, as it has been reported that platinum resistance might have resulted from enhanced tolerance [20], reduction in the adducts formation [18], and enhanced DNA damage repair [18].

4.5 In proteomics study involving 2 D gel electrophoresis:

 doi:10.20944/preprints202008.0667.v1

A total of 133 spots were identified, out of which 101 proteins were significantly altered in expression. Among them, 54 spots were successfully identified by MS. In some cases, mass spectral analysis showed that the same protein was named for more than one spot such as spots 16 ,18 and 76 were assigned to hnRNPA2/B1, spots 17 and 31 were assigned to ENOA, spots 52 and 63 were assigned to EF2, and spots 36 and 96 were assigned to VIME. Assignment of different spots to the same protein that exists in multiple isoforms with different *pI*s, might be attributed to the post-translational modifications, which was suggested to occur in 2-D gel electrophoresis-based proteomics studies [21,22], thus reducing the total to (49) proteins. Based on the protein functions, proteins differentially expressed in A2780^{cisR} cell line were divided into nine major groups as discussed in the next section using A2780 and A2780^{cisR} cell lines alternatively as a reference, also are illustrated in table 11-12.

 doi:10.20944/preprints202008.0667.v1

361 1.

Table 11 Functional classification of the proteins that differentially expressed in A2780^{cisR} cell line compared to A2780 cell line due to treatment using parent cell line A2780 as reference.

Match ID	A2780^{cisR} / A2780	Protein ID
Stress and chaperones		
3	DR	CYPA
32	ND	TCPB
35	DR	ERp57
39	ND	TCPH
45	DR	HSP7C
46	DR	mortalin
47	UP	BIP
51	DR	HSP90B
54	DR	GRP94
88	ND	Hop
105	ND	TCPA
Metabolism and biosynthetic processes		
11	ND	PGAM1
17/31	ND	ENOA
19	DR	LDHB
33	ND	SERA
55	DR	IMMT
63	DR	NM23
97	ND	ATPA
95	ND	PSAT
Cytoskeletal proteins		
5	DR	P18
36/96	UR	VIME
94	ND	GBLP
108	ND	CAH2
Initiation and elongation		
25	ND	EFTU
4	DR	EIF5A1
27	ND	EF1G
52	ND	EF2
mRNA Processing proteins		
15	UR	hnRNPA1
16/76	UR	hnRNP A2/B1

Table 12 Functional classification of the proteins that differentially expressed in A2780^{cisR} cell line compared to A2780 cell line due to treatment using A2780^{cisR} cell line as reference.

Match ID	A2780^{cisR} / A2780	Protein ID
Stress and chaperones		
44	DR	P4HB
57	UR	APG2
Metabolism and biosynthetic processes		
13	UR	TPI
8	UR	ATP5H
25	UR	GOT1
16	UR	VDAC1
41	UR	KPYM
Cytoskeletal proteins		
32	UR	ACTG
58	UR	VINC
Initiation and elongation		
30	UR	EF1A1
63	UR	EF2
mRNA processing proteins		
18	ND	hnRNP A2/B1
Detoxification and drug resistance		
22	UR	PGK1
Cell Cycle regulation and cell proliferation		
69	DR	CLIC1
Signal transduction and cell cycle		
9	UR	RAN
Protein synthesis and degradation		
12	UR	PSA7

*DR: Down-regulated

*UR: Up-regulated

*ND: Not-detected

 doi:10.20944/preprints202008.0667.v1

Detoxification and drug resistance		
8	ND	PRDX1
66	ND	PRDX6
Cell cycle regulation and cell proliferation		
7	DR	Op18
89	ND	MCM7
Signal transduction and cell cycle		
13	DR	1433Z
Protein synthesis and degradation		
69	DR	PSA3

*DR: Down-regulated

*UR: Up-regulated

*ND: Not-detected

362 2.

363

 doi:10.20944/preprints202008.0667.v1

364 ***Mortalin,*** also known as GRP75 [15], a member of chaperones and stress related
365 proteins which plays essential function in mitochondrial proteins folding, importing [23],
366 cancer cell proliferation, inhibition of apoptosis, and enhancement of angiogenesis [24]. In
367 this study, mortalin was found to be down-regulated in the cisplatin-resistant A2780^{cisR} cell
368 line as compared to the sensitive A2780 cell line when A2780 was used as a reference,
369 consistent with the earlier studies conducted in the host laboratory [25-27]. Collectively, the
370 findings indicate that mortalin may play a role drug resistance, representing mortalin as
371 potential diagnostic and therapeutic targets. Treatments with the synergistic combinations of
372 (CS and OA using 0/0 h) and (CS and ART using 0/0 h), partially restored mortalin
373 expression in A2780^{cisR} cell line, suggesting that the applied treatments have improved
374 mortalin chaperones action towards greater cell kill.

375 ***APG2*** is another molecular chaperone and stress related protein which also known
376 as HSP74 [15], that is ubiquitously expressed in different organs [28]. In this study APG2 was
377 over-expressed in the cisplatin-resistant A2780^{cisR} cell line as compared to the sensitive
378 A2780 cell line. Up-regulation of APG2 expression was previously reported in
379 hepatocellular carcinomas [28]. The elevated expression was related to drug resistance, poor
380 prognosis or advanced stages in different type of cancers [28]. The findings indicate that
381 APG2 plays a role in the development of drug resistance owing to its action as heat-shock
382 protein preventing the stress caused by platinum drugs, suggesting that APG2 can be a
383 potential prognostic and therapeutic target. APG2 expression was lowered below threshold
384 of detection after treatment with synergistic combinations of (CS and ART using 4/0 h), (CS

and OA using 0/4), (CS and ART using 0/0 h) and (CS and OA using 0/0), that might have inhibited its behaviour as heat shock protein exposing cells to the toxic effect of CS thereby increased cell apoptosis, indicating a causal relationship between APG2 expression and platinum resistance in ovarian cancer.

BIP also known as GRP78 [15], is involved in protein biosynthesis. Kang et al. reported that BIP was over-expressed in a large number of cancers, including malignant gliomas, lung cancer, and breast cancer [29]. It enhances tumour metastasis, survival, proliferation, and resistance to a wide range of therapies [30], including cisplatin [31]. Stimulation of the BIP expression plays as a defense mechanism to protect cancer cells against certain stress conditions [31]. In line with the reported findings, in the present study, BIP was up-regulated in the A2780^{cisR} cell line as compared to A2780 cell line when A2780 was used as a reference. Taken together, these findings indicate that BIP alteration plays a significant role in the development of the drug resistance and poor outcome. Treatment with selected combinations, over-restored BIP expression, indicating that the treatments have prevented BIP roles of cell protection and the tumorigenicity of cancer cells and thereby increased the death of cells exposed to CS, suggesting that the selected combinations can serve as alternative therapeutic methods for the resistance in ovarian cancer associated with abnormal BIP expression. Thus, it would seem to suggest that BIP may possibly be playing a major role in these synergistic outcomes.

HSP90B (also known as HS90B) [15] is one of the HSP90 isoforms found in mammalian cells [32,33]. HSP90 is involved in the differentiation and cell proliferation

406 processes [34]. It exhibits an anti-apoptotic effect through the modulation of NF-κB, TNF,
407 and AKT pathways. It enhances tumour growth and angiogenesis through the VEGF
408 pathway [35]. HSP90B was reported to be associated with development of multidrug
409 resistance [34]. In the present study, HSP90B was down-regulated in the cis-resistant cell
410 line as compared to A2780 cell line when A2780 was used as a reference, consistent with the
411 findings of earlier studies at the host laboratory [21,26,27].The findings indicate that HSP90B
412 plays an important role in apoptosis pathway and in the development of drug resistance.
413 Therefore, it can be a promising diagnostic and therapeutic target. HSP90B expression was
414 partially / over-restored after the treatment with the selected combinations, possibly be due to
415 the effect of the treatments on HSP90B capability to interact with survival signal, including
416 NF-κB and AKT, leading to their inactivation thereby sensitizing cells to apoptosis mediated
417 by the stresses produced by CS. Hence restoration of HSP90B can be a contributing factor
418 responsible for apoptosis enhancement so that the level of its expression can be a means for
419 drug resistance in ovarian cancer.

420 ***GRP94*** also known as ENPL [15], is a member of hsp90 family. The high level of
421 GRP94 expression was found in many cancers such as breast, gastric, esophageal, colon,
422 lung, and breast cancer [36]**.** However, in the present study, GRP94 was down-regulated in
423 the cisplatin-resistant A2780^{cisR} cell line as compared to A2780 cell line when A2780 was
424 used as a reference. The result is consistent with the findings of earlier studies at the host
425 laboratory [21,25,27]. Collectively, these findings suggest that GRP94 expression is a cell and
426 cancer dependent and suggest GRP94 as potential diagnostic and therapeutic target.

Treatment with selected combinations over-restored GRP94 expression. Together with the fact that the GRP94 as one member of HSPs family protects cells from stressful stimuli, suggests that this protein could play a role in tumorigenicity and drug resistance in ovarian. Thus, the result supports the possibility of a causal relationship between GRP94 expression and the resistance caused by CS.

CYPA is one of CyPs isoforms (also known as PPIA) [15]. CYPA catalyzes cis-trans isomerization of the peptide bonds [15,37]. CYPA is up-regulated in glioblastoma multiforme, melanoma, colorectal, breast and pancreatic cancer [38]. In contrast, CYPA in the present study was down-regulated in the cis-resistant cell line as compared to the sensitive A2780 cell line when A2780 was used as a reference, this is consistent with the findings of the earlier studies conducted at the host laboratory [26,27]. The results suggest that CYPA is involved in drug resistance in ovarian cancer, Treatment with synergistic combinations of (CS and ART using 4/0 h), (CS and OA using 0/4 h) (CS and ART using 0/0 h) partially-restored CYPA expression. While after treatment with (CS and OA using 0/0 h) CYPA expression was not detectable, suggesting that CYPA expression is very sensitive to the treatment. Where the enhanced apoptosis be brought about may be the result of OA's signalling inhibitory mechanism and its ROS production that have modulated CYPA activities of antioxidant stabilization, transcriptional control, trafficking, cell cycle regulation and signal transduction [39]. Thus, the results suggest that there is a strong correlation between CYPA expression and apoptosis, thus the chosen treatments can serve as potential approaches to overcome drug resistance associated with atypical CYPA expression.

 doi:10.20944/preprints202008.0667.v1

P4HB is one member of PDI family also known as PDIA1 [15], It has multifunctional activities besides its involvement in the disulfides breakage, formation and rearrangement at different cellular locations [40]. P4HB is up-regulated in glioblastoma cancer [41]. Silencing of P4HB inhibits tumour survival of MCF-7 cells, however it did not show a significant inhibitory effect on HeLa cells [41]. Thus, it has been suggested that P4HB expression is a cell-type dependent [41]. In the present study, P4HB was down-regulated in A2780^{cisR} cell line as compared to sensitive A2780 cell line when A2780^{cisR} was used as a reference. The result is in accordance with the previous findings of the earlier studies conducted at the host laboratory [21,25,27]. The data clearly supports P4HB roles in cancer progression and resistance, while its expression is cell and cancer-dependent. Thus, P4HB expression can be a strong prognostic indicator that might also be a potential therapeutic target. Treatment with synergistic combinations of (CS and OA using 0/0 h) over-restored P4HB expression. Whereas, treatment with synergistic combinations of (CS and ART using 0/0 h) partially-restored P4HB expression, suggesting the involvement of P4HB in apoptotic pathway and indicating that the rise in growth inhibition was caused by the increased P4HB expression. Therefore, the selected combinations are effective in overcoming drug resistance in ovarian cancer model.

ERp57 is another member of the PDI family, which also known as Erp60, PDIA3 and GRP58 [15], is a chaperone, oxidoreductase and disulfide isomerase protein [42]. ERp57 plays a crucial role along with CRT and CNX chaperones in folding process of disulfide bond-containing proteins and highly glycosylated [43]. It reacts with Ref-1 and STAT3, and

involved in the formation of STAT3–DNA complexes [44]. Although, ERp57 was reported to be up-regulated in cervical [41], liver, breast, rectal, thyroid and gastric cancer [45]. It was significantly decreased in the most of metastases and primary gastric cancers [46]. Similarly, in this study, ERp57 was down-regulated in cis-resistant cell line as compared to the sensitive counterpart cell line, when A2780 was used as a reference. Thus, the result together with literature data, indicate that dysregulation of the ERp57 expression enhances drug resistance and cancer progression while its level of expression is highly dependent on cell and cancer type. Hence, ERp57 may serve as a beneficial diagnostic marker and therapeutic target. Treatment of $A2780^{cisR}$ cell line with synergistic combination of (CS and OA using 0/0 h) over-restored ERp57 expression while (CS and ART using 0/0 h) partially restored its expression, indicating a causal relationship between ERp57 expression and platinum resistance in ovarian cancer.

PGAM1 also known as PGAMA [15], is a glycolytic enzyme that converts 3-PG to 2-PG with 2, 3-BPG for energy production [47]. PGAM1 was over-expressed in different types of cancer such as hepatocellular carcinoma, breast carcinoma and colorectal cancer [47]. In the present study, PGAM1was not detected in $A2780^{cisR}$ cells as compared to sensitive counterpart cell line when A2780 cell line was used as a reference, possibly due to low concentration or detection problems. Given the important role of PGAM1 in the energy production associated with cell growth and cell proliferations, suggesting that PGAM1 may possibly be serving as a potential biomarker and therapeutic means towards Pt-resistance in ovarian cancer. Treatment with synergistic combination of (CS and ART using 4/0 h) over-restored PGAM1 expression. while treatment with synergistic combinations of (CS and

 doi:10.20944/preprints202008.0667.v1

ART using 0/0 h) partially restored PGAM1 expression. Whereas, after treatment with synergistic combinations of (CS and OA using 0/0 h) and (CS and OA using 0/4 h) PGAM1 expression was below threshold of detection. The results imply that level of PGAM1 expression was extremely sensitive towards the treatments that inhibited its ability to produce energy to nourish cancer cells thereby increased their vulnerability to the platinum drug. Hence, restoration of PGAM1 can be a contributing factor responsible for apoptosis enhancement so that the level of its expression can be a means for drug resistance in ovarian cancer. Therefore, chosen combinations can be helpful in sensitizing resistant cells towards platinum drugs and decreasing their side effects.

LDHB also known as LDH-H [15], is involved in conversion of lactate to pyruvate [48]. LDHB was reported to be over-expressed in archival metastatic melanoma [49] and nasopharyngeal carcinoma [50]. However, it was found to be down-regulated in the MHCC97-H hepatocellular carcinoma cell strain against less metastatic MHCC97-L cell strain [51], and in the highly metastatic gallbladder carcinoma (GBC-SD18H) versus (GBC-SD18L) less potential metastasis cell line [52]. Similarly, in this study LDHB was down-regulated in A2780^{cisR} cell line as compared to sensitive counterpart cell line when A2780 was used as a reference, The findings indicate that aberrant LDHB expression is cell, stage and cancer type dependent, hence, targeting LHDB expression level would be beneficial diagnostic and therapeutic strategies. LDHB expression was partially /over-restored after treatment with the chosen combinations, supporting the idea that synergistic outcomes, besides other reasons are associated with enhancement of CS cytotoxic

effects by ART and OA through LHDB restoration which have modulated its role in energy metabolism, suggesting a strong correlation between LDHB expression and apoptosis improvement.

ATPA, also known as ATP5A1, is a mitochondrial enzyme involved in the synthesis of ATP from ADP [15]. Over-expression of ATPA expression was observed in breast cancer cell (MCF7) [53], anaplastic thyroid cancer [54], acute lymphoblastic leukemia [55], multidrug resistant cervical carcinoma (MDR) KB-v1 cells [56], and resistant leukaemic cells [57]. However, ATPA expression was down regulated in clear cell renal cell carcinoma [58], and chromophobe renal cell carcinoma [59]. In this study, ATPA was not detectable in $A2780^{cisR}$ cell line as compared to its sensitive counterpart when A2780 was used as a reference, possibly due to low concentration. The findings suggest that the dysregulation of ATPA level contributes to carcinogenesis event and targeting this protein might be of therapeutic importance.Treatment with synergistic combinations of (CS and OA using 0/4 h) and (CS and ART using 4/0 h) over restored its expression. ATPA expression after treatment with synergistic combinations of (CS and ART using 0/0 h) and (CS and OA using 0/0 h) was not detectable, suggesting that the nominated combinations are extremely effective in overcoming drug resistance in ovarian cancer model.

ATP5H "generates ATP from ADP in the existence of a proton gradient throughout the membrane." [15], ATP5H is overexpressed in lung adenocarcinomas [60] and MCF7 cell line [53]. Consistent with the reported findings, in the current study, ATP5H expression was up-regulated in $A2780^{cisR}$ cell line as compared to the level found in sensitive A2780 cell line

 doi:10.20944/preprints202008.0667.v1

when 2780^{cisR} cells were used as a reference. These data point to the contribution of ATP5H in cancer formation and suggest that ATP5H may serve as a possible diagnostic marker and molecular target. ATP5H expression after the treatment with synergistic combinations of (CS and OA using 0/4 h), (CS and ART using 4/0 h), (CS and OA using 0/0 h) and (CS and ART using 0/0 h) was not detectable, suggesting that ATP5H expression is very sensitive to the combinations. Hence, these combinations would in helpful in opposing resistance in ovarian cancer.

TPI also known as TIM [15], is involved in the pathway of energy metabolism through catalyzing the interconversion of DHAP to GAP [61]. TPI expression level was over-expressed in bladder squamous cell [61], prostate, lymph node, kidney, skin, testis, stomach, brain [62], epithelial ovarian cancer paclitaxel resistant A2780TC1 cells versus its sensitive cell line [63], and hepatocellular carcinoma versus normal tissues [47]. This is consistent with the current study wherein TPI was up-regulated in ovarian cancer cis-resistant versus its sensitive cell line using A2780^{cisR} cell line as reference. The findings suggest that dysregulation of TPI expression is playing a role in cancer promotion and drug resistance. Thus, it can be said that TPI can serve as potential biomarker and therapeutic targets. Treatment of A2780 cell line with synergistic combination of (CS and ART using 0/0 h) over-restored TPI expression. While treatment of A2780^{cisR} cell line with synergistic combination of (CS and ART using 4/0 h) partially restored its expression. Whereas, treatment with synergistic combination of (CS and OA using 0/0 h) fully-restored its expression, suggesting a strong correlation between TPI expression and improved cell kill.

 doi:10.20944/preprints202008.0667.v1

555 ***GOT1,*** alternatively named as AATC [15], catalyzes the interconversion of
556 α-ketoglutarate and aspartate to glutamate and oxaloacetate [64]. Yu et al. reported that the
557 elevation of GOT1 expression in pancreatic cancer was associated with shorter overall
558 survival rate [65]. Similarly, Chakrabarti, G. reported that the elevated level of GOT1 in
559 NSCLC resulted in poor outcome after radiotherapy was given, suggesting its involvement in
560 the development of radio-resistance [66]. The same, in this study, GOT1 was up-regulated in
561 cis-resistant cell line as compared to its sensitive A2780 cell line using $A2780^{cisR}$ cell line as
562 reference, suggesting GOT1 involvement in the development of drug resistance thus, it can
563 be promising therapeutic and diagnostic tool. Treatment with synergistic combinations of
564 (CS and ART using 0/0 h) partially-restored GOT1 expression. After treatment with
565 synergistic combinations of (CS and OA using 0/0 h), (CS and OA using 0/4 h) and (CS
566 and ART using 4/0 h), GOT1 expression was not detectable, suggesting that GOT1 is highly
567 sensitive towards the treatments. Thus, it may play a major role in the synergistic outcomes,
568 implying a causal relationship between GOT1 expression and drug resistance.

569 ***NM23***, relatively named as NDKA [15], is considered as metastasis-suppressor [67].
570 It is involved in large numbers of different biological activities [68], including cell migration,
571 growth control, differentiation and signal transduction [67]. NM23 level was down-regulated
572 in metastasis ovarian carcinoma [69] and nasopharyngeal carcinoma [70]. Likewise, in this
573 study NM23 was down-regulated in $A2780^{cisR}$ cell line as compared to the level found in
574 sensitive A2780 cell line using A2780 cell line as reference, suggesting that down regulation
575 of NM23 plays a role in apoptosis inhibition, pointing out that NM23 expression can be a
576 prognostic marker and therapeutic target. Treatment with synergistic combinations of (CS

 doi:10.20944/preprints202008.0667.v1

and ART using 0/0) partially-restored NM23 expression. NM23 expression was not detectable after the treatment with the synergistic combinations of (CS and OA using 0/0 h), (CS and OA using 0/4 h) and (CS and ART using 4/0 h), suggesting that its expression is strongly sensitive towards the treatments. Thus, the combinations are beneficial in overcoming drug resistance involving abnormal NM23 expression.

IMMT, also known as Mic60 [71]. It promotes protein import via (MIA) pathway and regulates cristae morphology and crista junctions [71]. It found to be down-regulated in prostate cancer androgen-independent (DU145) versus androgen-dependent (LNCaP) cell lines [72]. Similarly, in this study, IMMT expression was decreased in cis-resistant cell line as compared to its sensitive cell line using A2780 cell line as reference, suggesting its usefulness as biomarker for platinum resistance in ovarian cancer. Treatment with synergistic combinations of (CS and ART using 0/0 h) and (CS and OA using 0/0 h) partially restored IMMT expression, suggesting that IMMT may be is playing a role in those synergistic outcomes, given that with the elevation of IMMT expression cell death was increased. Generally, this could be partly attributed to OA and ART actions which adjusted the molecular pathways including increasing Bax, decreasing Bcl-2, up-regulating of the caspases, and down-regulating NF-κB pathway thereby increased cell sensitivity towards platinum compounds leading to a greater growth inhibition. Therefore, the selected combinations can be a helpful in overcoming drug resistance involved abnormal IMMT expression.

KPYM, also known as PKM2 and PKM [15], catalyzes the conversion of phosphoenolpyruvate to pyruvate [73]. It is one member of PK family [74], that plays an essential role in tumour growth and metabolism process [74], through its aerobic glycolysis ability [75]. KPYM was down-regulated in gastric carcinoma in cis- resistant cell line versus its sensitive cell line [76] and in colorectal cancer OX-resistant cell line versus its sensitive cell line [77]. However, up-regulation of KPYM was reported in other type of cancers, including multiple myeloma, renal cell carcinoma, pancreatic cancer, ovarian, lung [74], breast, and colon cancer [78]. Likewise, KPYM in this study, was up-regulated in cis-resistant cell line versus its sensitive cell line using A2780^{cisR} cell line as reference. The results indicate that KPYM expression is cell and cancer type dependent and its expression is potential diagnostic and therapeutic targets. Treatment with synergistic combinations of (CS and ART using 0/0 h) and (CS and OA using 0/0 h) partially-restored KPYM expression. Whereas, after treatment with synergistic combinations of (CS and OA using 0/4 h) and (CS and ART using 4/0 h) KPYM expression was not detectable, implying that KPYM is very sensitive to the indicated combinations, suggesting a strong connection between enhanced apoptosis and KPYM expression.

PSAT, also known and SERC [15], catalyzes the formation of 3-phosphoserine from 3 phosphohydroxypyruvate [79], besides its involvement in serine biosynthesis [80]. The elevated expression of PSAT was observed in some cancer types, for example, in colon cancer [80] and clear cell ovarian carcinoma [81]. However, PSAT was not detectable in A2780^{cisR} cell line as compared to its parental cell line using A2780 as a reference, this could be attributed to the detection issue or low concentration. After treatment synergistic

 doi:10.20944/preprints202008.0667.v1

combinations of (CS and ART using 4/0 h) and (CS and OA using 0/0 h) PSAT expression was over-restored, suggesting that PSAT may be is participating in the final outcomes where the apoptosis initiation may perhaps be related to improvement of PSAT expression. Thus, the present data may point out PSAT as potential diagnostic and therapeutic targets.

VDAC1, (also known as porin 31HM [15], regulates metabolic homeostasis and cell energy [82]. It interacts with antiapoptotic regulators (hexokinase, Bcl-Xl and Bcl-2). It is involved in releasing apoptotic factors presented in the mitochondria [82]. High level of VDAC1 was observed in various cancers, including cervical, lung, pancreatic, ovarian and thyroid cancers [83]. Likewise, in this study, VDAC1 expression was up-regulated in cis-resistant cell line as compared to parental cell line using $A2780^{cisR}$ as a reference. The findings suggest that the VDAC1 is involved in tumour progression and that it may serve as useful biomarker and therapeutic target. After treatment with synergistic combinations of (CS and ART 4/0 h), (CS and OA using 0/4 h), (CS and ART 0/0 h) and (CS and OA using 0/0 h) VDAC1 expression was not detectable, suggesting that VDAC1 expression is significantly sensitive to the treatments. The result is implying that the rise in apoptosis could be attributed to a significant down-regulation of VDAC1 expression, suggesting a direct association between them, indicating the effectiveness of the selected treatments in restoring VDAC1 expression towards greater cell kill.

ENOA also known as Enolase 1 [15], is a metabolic enzyme which is implicated in pyruvate synthesis [84]. It facilitates the stimulation of extracellular matrix degradation and plasmin acting as a plasminogen receptor to promote tumour metastasis [84,85]. ENOA was elevated in in several malignancies, including breast, brain, gastric, cervix, colon, and kidney

 doi:10.20944/preprints202008.0667.v1

641 [84]. However, in the present study, ENOA was not detectable in the A2780^{cisR} cell line as
642 compared to its sensitive cell line using A2780 as a reference. Similarly, four previous
643 findings from the host laboratory reported the same finding [21,25-27], implying that ENOA is
644 playing a significant role in development of platinum resistance in ovarian cancer. ENOA
645 expression was over /partially-restored due to treatment with the selected combinations. It
646 can thus be suggested that the treatments have inhibited ENOA ability to stimulate
647 extracellular matrix degradation that has enhanced apoptosis induction. In general, therefore,
648 it seems that the enhanced apoptosis could be to some extent ascribed to OA and ART
649 pro-apoptotic ability to down-regulate NF-kB and Bcl-2 together with their cellular
650 regulatory functions, that in turn has improved cancer cells sensitivity to CS thereby
651 enhanced apoptosis induction.

652 ***VIME*** is class 3 of intermediate filaments family [15,86]. It is associated with
653 tumorigenesis, progression and initiation of cancer [87]. VIME is up-regulated in different
654 type of cancers such as lung, breast, prostate and colorectal [87]. Consistent with the reported
655 findings, VIME was up-regulated in cisplatin-resistant A2780^{cisR} cell line as compared to its
656 sensitive cell line using A2780 cell line as reference. The results indicate that VIME is
657 playing a major role in cancer progression and reveal that VIME expression can be a valuable
658 marker for various cancers. Treatment with synergistic combinations of (CS and OA using
659 0/4 h) over-restored its expression in the A2780 cell line. Likewise, treatment with
660 synergistic combinations of (CS and ART using 0/0 h) and (CS and OA using 0/0 h)
661 over-restored the VIME expression. It can thus be suggested that the synergism and observed

improve in apoptosis is directly dependent on VIME manifestation. Where the treatments were effective in preventing its cell protection role, given that VIME provides resistance against stress and maintains cellular integrity [86]. Therefore, the nominated combinations can serve as useful means to sensitize cancer cells towards CS therapy.

CAH2 is involved in extracellular acidification [88]. CAH2 was up-regulated in pancreatic and nervous system tumours [89], gastric carcinomas, and brain tumours [90]. In contrast, down regulation of CAH2 was reported in colorectal tumours [89] and hepatocellular carcinoma [90]. In this study, CAH2 was not expressed in $A2780^{cisR}$ cell line as compared to its sensitive counterpart using A2780 as a reference, that may be due to low concentration or detection problems. Altogether, the findings suggest that the aberrant expression of CAH2 plays a role in cancer formation, metastasis, and resistance to chemotherapy, thus it can serve as a promising diagnostic biomarker and therapeutic target. CAH2 expression was extremely sensitive to the treatment with synergistic combinations of (CS and ART using 4/0 h), (CS and OA using 0/4), (CS and ART using 0/0 h) and (CS and OA using 0/0), Which might have modulated its acidification regulation activity in response to hypoxic environment leading to decrease cell proliferation that ultimately has increased cell death. Therefore, the results suggest that the restoration of CAH2 expression can be one of the causal factors for apoptosis induction. Thus, chosen combinations can be effective in combating drug resistance in ovarian cancer involving abnormal CAH2 expression.

VINC is located in cell-adherence junctions and in focal adhesions [91]. It influences adhesion protein turnover and contractility as well as regulates the cell signaling processes

 doi:10.20944/preprints202008.0667.v1

683 [91]. Vinculin may act as a metastasis inhibitor by decreasing cell motility and tumour
684 inhibitor by assisting anchorage-dependent cell growth [91]. In this study, VINC was
685 up-regulated in the cisplatin-resistant A2780^{cisR} cell line as compared to its sensitive
686 counterpart using A2780^{cisR} cell line a reference, the result suggests the VINC expression as
687 potential therapeutic and diagnostic approaches. Treatment with synergistic combinations of
688 (CS and ART using 0/0 h) and (CS and OA using 0/0 h) partially-restored its expression in
689 A2780^{cisR} cell line. Whereas, after treatment with synergistic combinations of (CS and ART
690 using 4/0 h) and (CS and OA using 0/4 h) the expression of VINC was not detectable because
691 of the effect of treatments, which by restoring its expression may be altered protein turnover
692 towards a greater protein degradation thereby enhanced growth inhibition. Hence, the result
693 suggests that the significant reduction in VINC expression can be a causative factor
694 accountable for improved growth inhibition.

695 ***GBLP*** also known as RACK1 [15], is a cytosolic protein [92,93] which can interact
696 with STAT, tyrosine kinases/phosphatases, PDE4D5, and PKC pathways, involved in cell
697 movement, growth, division and adhesion [92]. GBLP was over-expressed in non-small cell
698 lung cancer, melanoma and hepatocellular carcinoma [92]. In the present study, GBLP was
699 below threshold of detection in the A2780^{cisR} cell line as compared to sensitive A2780 cell
700 line using cell line A2780 as reference. GBLP expression was over-restored due to the
701 treatment with the selected combinations, suggesting that GBLP restoration is playing a
702 contributory role in enhanced apoptosis resulting from chosen combinations which might
703 have adjusted its behavior thereby hindered the cell movement cell division towards a batter

704 growth inhibition. It is likely that the significant improve in GBLP expression is directly
705 associated with increased cells receptivity, suggesting GBLP as valuable diagnostic and
706 therapeutic target.

707 ***p18*** also known as COF1 is a member of COF family [15]. It controls actin dynamics
708 involved in micropinocytosis, chemotactic movement, cell migration, phagocytosis, and
709 proliferation [94]. Over-expression of p18 was reported in radioresistant astrocytomas [94,95],
710 pancreatic cancer versus non-cancerous tissues [94], In this study, however, p18 was
711 down-regulated in cis-resistant cell line as compared to its sensitive counterpart using A2780
712 as a reference. Although, the result is inconsistent with the reported findings, it can be said
713 that this maker would be promising diagnostic and cancer therapeutic target given its
714 important role in cell movement and propagation. After treatment with synergistic
715 combinations of (CS and ART using 4/0 h) and (CS and OA using 0/4 h) (CS and ART using
716 0/0h) partially-restored p18 expression, suggesting that the observed increase in apoptosis
717 level could be attributed to partial restoration of p18 expression. This may imply that p18 is
718 possibly be involved in development of platinum resistance in ovarian cancer, taken into
719 consideration its vital role as a member of cofilin family.

720 ***EIF5A1*** also known as IF5A1 [15], is one isoforms of hypusinated eIF5A. It is an
721 essential protein that undergoes many PTM, including acetylation and hypusination [96], that
722 involved in cell proliferation and translation elongation stage [96]. EIF5A1 up-regulated in
723 several malignancies, including colorectal carcinoma, lung adenocarcinoma and
724 glioblastoma [97], for that reason EIF5A1 considered a tumour promoter (oncogene). In this
725 study, EIF5A1 was down-regulated in cis-resistant cell line as as compared to the level found

 doi:10.20944/preprints202008.0667.v1

726 in sensitive A2780 cell line using A2780 cell line as a reference. In support of this, Scuoppo
727 et al. reported down-regulation of EIF5A1 in lymphoma [98] and knocking down of EIF5A1
728 has promoted the tumorigeneses of lymphoma, suggesting it as a tumour suppressor [98]. The
729 findings suggest that EIF5A1 is playing a role in apoptosis inhibition and that its expression
730 is cancer and cell-type dependent. After treatment the A2780^{cisR} cell line with synergistic
731 combinations of (CS and ART using 0/0 h) and (CS and OA using 0/0 h) EIF5A1 expression
732 was partially-restored, suggesting that the treatments were able to interrupt its role in protein
733 biosynthesis thereby prevented translation leading to cells death. Therefore, the results
734 suggest a causal relationship between EIF5A1 expression and platinum resistance in ovarian
735 cancer. Hence, the selected combinations can serve as useful treatments to sensitize cancer
736 cells towards platinum therapy.

737 ***EF2*** is one member of elongation group, involved in protein translocation in
738 elongation stage [99]. EF2 was over-expressed in colorectal and gastric cancers [99], and that
739 was suggested to be due to EF2 ability to stimulate the cell cycle progression at G2/M, cdc2
740 and Akt resulting in cells growth enhancement [99]. The result of the present study agrees
741 with the above finding, EF2 was over-expressed in A2780^{cisR} cell line as compared to A2780
742 cell line using A2780^{cisR} cell line as reference. The findings together with the important role
743 of EF2 in protein biosynthesis, clearly supports the idea that elevation of EF2 expression is
744 possibly be involved in ovarian cancer progression and drug resistance. Hence, the results
745 represent EF2 as new promising diagnosis biomarker and therapeutic target. Treatment, with
746 synergistic combinations of (CS and OA using 0/4 h) and (CS and ART using 4/0 h)
747 partially-restored EF2 expression. After the treatment with synergistic combination of (CS

 doi:10.20944/preprints202008.0667.v1

and ART using 0/0 h) EF2 expression was over-restored. This suggests that the observed rise in apoptosis degree is attributed to improvement of the CS cytotoxic effects by ART and OA actions towards opposing the drug resistance in ovarian cancer, indicating a causal relationship between EF2 expression and platinum resistance in ovarian cancer.

EFTU is another member of elongation proteins family, [15]. It regulates the phosphatidylinositol 4,5 bisphosphate and phosphatidylinositol 4-phosphate levels [100]. EFTU was reported to be up-regulated in stomach, oesophageal, pancreatic, lung and renal tumours [101]. In this study EFTU was not expressed in A2780^{cisR} cell line as compared its sensitive counterpart using A2780 was used as a reference, consistent with this Srisomsap et al. reported that EFTU was not expressed in HepG2 cell line [102] Altogether, the findings indicate that EFTU expression is cancer and cell type dependent, suggesting that the EFTU expression can be a potential biomarker and therapeutic target. Treatment with synergistic combinations of (CS and OA using 0/0 h), partially-restored EFTU expression level, while treatment with synergistic combination of (CS and ART using 0/0 h) over-restored its expression, indicating that the treatment could be an effective way to sensitize cancer calls towards platinum compounds.

EF1G is another member of the elongation proteins**.** Over-expression of EF1G was observed in gastrointestinal tract malignancies [103], acute myelogenous leukemia [104], prostate, stomach, colon, lung and breast cancer [105]. However, it was down-regulated in pancreatic cancers [106]. In this study, EF1G was not detectable (below threshold of detection) in A2780^{cisR} cell line as compared to the level found in sensitive A2780 cell line using as a reference. Taken together, the balance of evidence suggests that the EF1G expression is

possibly be cancer or/and cell type dependent, suggesting that targeting EF1G might be of therapeutic importance. Treatment with synergistic combinations of (CS and ART using 0/0 h) and (CS and ART 4/0 h) partially-restored EF1G expression, whereas, synergistic combination of (CS and OA using 0/4 h) over-restored its expression, suggesting that the restoration of EF1G by the treatments might have inhibited transformation by preventing translation of proteins during protein biosynthesis that have a direct role on cell growth reduction. Hence, EF1G expression may be is directly participating in the synergistic outcomes resulting from the combination of CS with OA and ART, where the improved apoptosis could be directly linked to EF1G restoration. Thus, selected combinations are effective in improving cancer cell sensitivity towards platinum drugs involved EF1G irregular expression.

EF1A1 is the other member of this group, involved in protein synthesis during elongation stage [107], that is also known as EEF1A1 [15]. **EF1A1** is associated with binding of G-actin, binding of microtubules, bundling of F-actin and transporting β-actin mRNA [107]. It is over-expressed in pancreatic melanoma, lung, breast, colon and prostate tumours [107]. Consistent with the reported findings, in the present study EF1A1 was up-regulated in A2780^{cisR} cell line as compared to its sensitive counterpart using A2780^{cisR} was used as a reference. The findings suggest that EF1A1 plays an important role in apoptosis inhibition and development of drug resistance. After treatment with synergistic combinations of (CS and OA using 0/4 h) and (CS and ART using 0/0 h) EF1A1 expression was over-restored. While treatment with synergistic combination of (CS and OA using 0/0 h) partially-restored its expression, suggesting a straightforward connection between the elevated growth

 doi:10.20944/preprints202008.0667.v1

inhibition and decreased EF1A1 expression. This clearly supports that targeting EF1A1 can be a promising means to increase cancer cells sensitivity towards platinum drugs. Hence, selected treatments can serve as alternative approaches to overcome Pt-resistance through improving EF1A1 expression.

hnRNPA1, belong to mRNA processing proteins, that plays fundamental functions in gene expression regulation at translational and transcriptional levels [108], also are implicated in cell signaling, telomere biogenesis and DNA repair [108]. ***hnRNPA1*** also known as ROA1 [15], is up-regulated in a large number of cancers such as colorectal, breast, gliomas and lung [109]. Similarly, in this study, hnRNPA1 was up-regulated in A2780^{cisR} cell line as compared to the level found in A2780 cells when A2780 was used as a reference, indicating that hnRNPA1 can be useful cancer biomarker and therapeutic target. Treatment of with synergistic combinations of (CS and ART using 0/0) and (CS and OA using 0/0) over-restored its expression. While after treatment with combinations of (CS and ART using 4/0) and (CS and OA using 0/4) hnRNPA1 expression was not detectable. Hence, the result suggests that the selected combinations have affected hnRNPA1 actions in gene expression and DNA repair thereby increased cells vulnerability to CS cytotoxic action leading to a better cell kill.

hnRNPA2/B1, also known as ROA2 [15], is another protein belongs to this group. It involves in various functions, including the regulation of mRNA metabolism, translation and transcription [110]. Up-regulated in serval cancer types such as pancreatic, lung [111] and breast [112]. Likewise, hnRNPA2/B1 was up-regulated in cis-resistant cell line as compared to the level found in sensitive A2780 cell line. Altogether, the findings indicate its

 doi:10.20944/preprints202008.0667.v1

814 therapeutic value as diagnostic and medicinal target. it is worth noting that in this study
815 hnRNPA2/B1 was named by MS for three spots (16 and 76 when A2780 was used as
816 reference spot 18 when was A2780^{cisR} when used as a reference). After treatment with
817 selected combinations hnRNPA2/B1 expression was partially and over-restored, suggesting
818 that the restoration of hnRNPA2/B1 expression is possibly has altered its translation and
819 transcription action thereby increased cell death. Hence, the result supports the possibility of
820 a causal relationship between hnRNPA2/B1 expression and the resistance in ovarian caused
821 by CS treatment.

822 ***PGK1*** is participating in the glycolytic pathway and contributing in angiogenesis
823 events [113]. PGK1 was up-regulated in various cancers, such as multi-drug resistant ovarian
824 cancer, breast cancer, renal cancer, pancreatic carcinoma, and squamous cell carcinoma
825 [113-116]. Similarly, in the present study, PGK1 was up-regulated in A2780^{cisR} cells as
826 compared to the level found in sensitive A2780 cell line when A2780^{cisR} was used as a
827 reference. Thus, it can be said that PGK1 and its signalling genes can serve as future
828 prognostic markers. Treatment with synergic combinations of (CS and ART using 0/0h), (CS
829 and ART using 4/0h) and (CS and OA using 0/4 h) partially-restored PGK1 expression,
830 suggesting the treatments might have influenced PGK1 angiogenic function thereby
831 prevented nutrients and oxygen leading to a greater cell kill. However, its expression was
832 further up-regulated due to the treatment with synergistic combination of (CS and OA using
833 0/0 h). From the above findings, it remains difficult to clearly establish clear association
834 between PGK1 expression and enhanced cell kill and synergistic outcome. Hence, further
835 studies would be necessary to gain better insight.

 doi:10.20944/preprints202008.0667.v1

836 ***PRDX1***, also known as PAG [15], is an antioxidant [117]. Its function interchanges
837 from (peroxidase to a chaperone) with a high level of hydrogen peroxide [117]. Up-regulated
838 level of PRDX1 was found in lung ovarian, liver, breast, gallbladder, prostate and bladder
839 cancer [117]. In this study, PRDX1 was below threshold of detection in cisplatin-resistant
840 $A2780^{cisR}$ cells as compared to the level found in A2780 cells when A2780 was used as a
841 reference. However, Ren, Ye et al. reported a "relatively weak expression" of PRX1 in
842 laryngeal cancer (Hep2), liver cancer cell (SUN449) lymphoma leukemia (KOPN63) and
843 acute lymphoblastic leukemia (MOLT-4) cell lines[117]. The discrepancies, a result of
844 unknown effect of PRDX1 or/ and its interchangeable role between peroxidase and
845 chaperone functions. However, it can be said that PRX1 expression is cell, stage and cancer
846 type dependent, suggesting a potential role of PRDX1 as therapeutic target and useful
847 biomarker. Treatment with synergistic combinations of (CS and OA using 0/4 h) and (CS and
848 ART using 4/0 h) partially-restored PRDX1 expression, While. treatment with synergistic
849 combinations of (CS and OA using 0/0 h) and (CS and OA using 0/0 h) over-restored PRDX1
850 expression, suggesting that the chosen combinations have repressed its antioxidant effect and
851 enhanced its chaperone action towards a greater rate of growth inhibition. Thus, the result
852 suggests a direct association between PRDX1 expression and apoptosis induction. Hence, the
853 nominated combinations are beneficial in overcoming drug resistance in ovarian cancer
854 involved abnormal expression of PRDX1.

855 ***PRDX6***, (also known as 1-Cys PRX), is a bifunctional enzyme [118] where it has a
856 phospholipase A2 and glutathione peroxidase activities [118]. It is involved in tumour
857 metastasis, proliferation and protection [118], playing both anti cytoprotective or

 doi:10.20944/preprints202008.0667.v1

cytoprotective roles [119]. PRDX6 was up-regulated in various cancers such as breast [118], lung [119], and oesophageal cancer [61]. In the present study, PRDX6 was below threshold of detection, in the A2780^{cisR} cell line as compared to the level found in A2780 cells when A2780 was used as a reference, however, RDX6 was very sensitive to selected treatments, suggesting a direct association between promotion of apoptosis and PRDX6 level of expression. Given its bifunctionality, it is possible that targeting PRDX6 might be of therapeutic importance.

Op18, also known as STMN1 [15], is a highly conserved phosphoprotein involved in cell proliferation, morphogenesis, and differentiation [120]. It plays a role in the regulation of the microtubule filament system through microtubules destabilization [15]. Fang et al. reported that Op18 was over-expressed in different cancers, including osteosarcoma, lung, breast, and bladder [121]. In contrast, in this study, Op18 was down-regulated in cisplatin-resistant A2780^{cisR} cells as compared to its sensitive counterpart using A2780 as a reference. However, the result is in line with previous findings from the host laboratory using the same cell lines [21,25], suggesting that Op18 expression is a cell and cancer type dependent. Despite these discrepancies, it can be said that Op18 can serve as a potential biomarker for the resistance in ovarian cancer. Treatment with synergistic combination of (CS and ART using 0/0 h) over-restored Op18 expression, suggesting the selected treatment may be have disturbed its morphogenetic signaling prevented cell proliferation that in turn led to growth inhibition, indicating that treatment could be an effective means to sensitize cancer calls towards cisplatin.

 doi:10.20944/preprints202008.0667.v1

879 ***MCM7,*** also known as CDC47 [15], is a member of the MCM complex [122]
880 involving in the regulation of cell cycle progression and licensing DNA replication [123].
881 MCM7 was over-expressed in different human cancers, including neuroblastoma, colorectal
882 and prostate [122]. In this study, MCM7 was not detected, below threshold of detection in
883 A2780^{cisR} cell line as compared to the level found in sensitive A2780 cell line when A2780
884 was used as a reference. Treatment with the synergistic combinations of (CS and OA using
885 0/0 h) over-expressed MCM7 expression. While treatment with the combination of (CS and
886 ART using 0/0 h) fully-restored its expression. This could be partially attributed to ART
887 inhibitory ability of the important cell cycle regulators, including CDK4, CDK2 [13], cyclin
888 A, cyclin E, cyclin D3, cyclin D1, CDK6 and E2F1 [17], given that MC7 is associated with
889 cell cycle regulation, it is possible that ART was able to recover MCM7 expression as a one
890 of the cell cycle regulators proteins, which in turn have improved CS cytotoxic action.
891 Therefore, the results suggest a direct correlation between improved cell death and MCM7
892 expression and indicate that the selected combinations are valuable in opposing of Pt
893 resistance in ovarian cancer.

894 ***CLIC1***, also known as NCC27 [15] is one of CLIC family which involved in the
895 regulation of trans-epithelial transport, cell volume, electrical excitability, pH levels, ion
896 homeostasis, cell adhesion, cells apoptosis and cell cycle [52]. In the present study, CLIC1
897 was down-regulated in cisplatin-resistant cell line as compared to the level found in sensitive
898 A2780 cell line when A2780^{cisR} cell line was used as a reference. Treatment with synergistic
899 combination of (CS and ART using 0/0 h) over-restored its expression, whereas, treatment
900 with synergistic combination of (CS and OA using 0/0 h) further down-regulated CLIC1

 doi:10.20944/preprints202008.0667.v1

expression. These obviously confusing findings suggest that CLIC1 may possibly not be playing any important role in those outcomes. However, taken into consideration CLIC1 role in chloride channel [124], cell adhesion, cells apoptosis and cell cycle [52], suggesting that targeting CLIC1 might be of therapeutic importance. Additional studies at molecular level would be required to clarify the matter.

RAN is a member of the Ras super-family [125], also known as GTPase Ran [15]. It promotes the assembly of bipolar spindle in mitosis phase [126]. The elevated level of RAN was reported in different cancers such as ovarian, stomach, kidney, colon and lung cancer [125]. Similarly, in this study, RAN was up-regulated in cis-resistant cell line as compared to its sensitive counterpart using $A2780^{cisR}$ cell line as reference. Silencing of RAN inhibited cell growth or/and induced apoptosis in colon, nasopharyngeal, renal breast and ovarian tumours [125]. The findings suggest that RAN expression is a promising diagnostic marker and therapeutic target. Treatment with synergistic combination of (CS and ART using 4/0 h) over-restored RAN expression, whereas, treatment with synergistic combinations of (CS and OA using 0/4 h), (CS and ART using 0/0 h) and (CS and OA using 0/0 h) partially-restored its expression, suggesting the treatments have suppressed RAN activity of bipolar spindle assembly in mitosis phase leading to a greater growth inhibition. Therefore, the results indicate that the reduction in RAN expression can be directly accountable for the observed rise in cell kill. Hence, the selected treatments can be a potential therapeutic strategy to sensitize ovarian cancer cells towards Pt drugs.

1433Z is another signal transduction protein, it is one isoform of the 14-3-3 family, that exhibits a pro-oncogenic role in multiple tumour types [127]. 1433Z is the key regulator

of the major cellular processes [128], including autophagy, progression, adhesion, differentiation, proliferation, and apoptosis [128]. 1433Z was down-regulated in A2780^{cisR} cells as compared to its sensitive counterpart, when A2780 was used as reference. Likewise, previous findings reported down-regulation of 1433Z in (A2780-TR, TA) paclitaxel-resistant as compared to its sensitive counterpart [129], and in (SKOV3-TR, TS) as compared to its sensitive counterpart [129]. However, up-regulation of 1433Z expression was reported with others cancers such as pancreatic [128], head and neck, NSCLC, breast [127], hepatocellular carcinoma, and stomach cancer [130]. Overall, the results indicate that 1433Z expression is cancer and cell dependent, suggesting that the level of its expression is a potential diagnostic marker for Pt-drug resistance in ovarian cancer, Treatment with synergistic combinations of (CS and ART using 0/0 h) and (CS and OA using 0/0 h) over-restored 1433Z expression, while treatment with synergistic combination of (CS and OA using 0/4 h) partially-restored its expression, suggesting that the growth inhibition produced by the combination of OA and ART with CS, was caused by the down-regulation of Bcl-2 and NF-κB mediated by other mechanisms. For example in the case of the combination with ART the final outcomes could be ascribed to the inhibition of cyclin A, cyclin E, cyclin D3, cyclin D1, CDK6, E2F1 and JAB1 transcriptions [17], CDK4, CDK2 expressions [13], S6K, PI3K, mTOR, Akt [10] and enhancement of IFIT3, p21, and p27 [17]. This has increased the influx of CS or/and decreased its efflux. Additionally, the selected combinations might have manipulated 1433Z effect on cell adhesion, cell differentiation, and cell proliferation which in turn has prompted apoptosis induction. Thus, the results overall suggest that the selected combinations are beneficial for 1433Z restoration towards overcoming drug resistance in ovarian cancer.

Two subunits of proteasome PSA3and PSA7 were also found to be differentially expressed, are involved in the regulation of several crucial cellular process, including apoptosis, immune responses, DNA repair, protein quality control and cell cycle progression [131]. PSA3 (also known as PSMA3) [15], was down-regulated in cis-resistant cell line as compared to its sensitive counterpart when A2780 was used as a reference, this is consistent with Moghanibashi et al. finding in which PSA3 was reported to be down-regulated in ESCC [132]. PSA7, also known as PSMA7 [15]. was up-regulated in cis-resistant cell line as compared to its sensitive counterpart when $A2780^{cisR}$ cell line was used as a reference. Up-regulation of PSA7 expression was reported previously in colorectal cancer [133]. The results suggest that PSA3 and PSA7 may serve as potential diagnostic and therapeutic targets. PSA3 and PSA7 expressions after treatment with selected combinations were either partially or over-restored, suggesting that the treatments may be have decreased PSA3 and PSA7 DNA repair ability and recovered their growth inhibition ability that have increased the cell cycle arrest and decreased protein quality control leading to a greater growth inhibition. Hence, the result suggests a causal relationship between PSA3 and PSA7 expressions and resistance to cisplatin therapy, signifying the effectiveness of the applied treatments in overcoming drug resistance involved abnormal PSA3 or/and PSA7 expression in ovarian cancer.

5. Materials and Methods

Materials and Methods

 doi:10.20944/preprints202008.0667.v1

CS, OA, ART, trypsin, Hepes, triton-X 100 , PBS, MTT, DMSO, and NaOH (Sigma-Aldrich, Australia), $K_2[PtCl_4]$ (Sigma, USA), KI (BDH Chemicals, Australia), A2780, $A2780^{cisR}$ and $A2780^{ZD0473R}$ ovarian cancer cell lines were kindly provided by Dr Philip Beale (NSW Cancer Centre, Royal Prince Alfred Hospital (RPAH), Sydney, Australia), Varian Cary 1E UV/VIS spectrophotometer, Varian SpectrAA240 atomic absorption (AAS) with GTA-120 graphite furnace tube atomizer at the host laboratory (School of Medical Sciences, The University of Sydney), 28% ammonia solution (UNIVAR, New Zealand), $AgNO_3$ (BDH Chemicals, Australia), FCS, 5X RPMI1640 media, L-glutamine, and $NaHCO_3$ (5.6%) (Thermo Trace Pty Ltd Melbourne, Australia), 25 cm^2 cell culture flasks (Crown Scientific), carbon dioxide incubator (SANYO, Japan), JETQUICK DNA Spin Kit (GENOMED GmbH, Germany), Tris (hydroxymethyl) aminomethane hydrochloride (Sigma, Germany), Calcusyn software version 2 (Bio-Rad, Cambridge, UK), urea and CHAPS (Calbiochem, Germany), thiourea and DTT (Merck, Germany). Melanie version 7.0 (SIB, Genebio, Switzerland). glycerol and SDS (MP Biomedicals, LLC, France), DeStreak reagent (GE Healthcare Bio-sciences AB, Sweden), criterion TGX Precast gel, iodoacetamide, carrier ampholytes, PROTEAN i12 IEF system, mineral oil, and 10 X tris/glycine buffer (Bio-Rad, USA), agarose, wicks, ChemiDoc XRS imaging system, Bio-Safe Coomassie Stain, ReadyStrip™ IPG Strip, criterion Dodeca cell, protein assay standard II kit, bromophenol blue, Microplate Reader Model 3550, and automated cell counter (Bio-Rad, Australia) 96 well flat bottom plates (Edward Keller), and KCl (BDH Chemicals, Australia).

Cell culture and subculture:

 doi:10.20944/preprints202008.0667.v1

Cell culturing was carried out following the same procedure as described previously [134]. Briefly, cells were grown in flasks 25 cm^2, incubated in 95% air, 5% CO_2 at 37°C. Cells were preserved in (log) growth phase in RPMI 1640 containing heat-inactivated fetal calf serum (10%), bicarbonate (0.112%), hepes (20 mM), and glutamine (2 mM). A2780 cell line was subjected to increasing intensity of CS until it gained resistant ($A2780^{cisR}$). Also, A2780 cell line was treated continuously with increasing strengths of ZD0473 to develop resistant to the drug [135].

Drugs preparation:

Cisplatin prepared according to the Dhara's method [136], was dissolved in dimethyl formamide (DMF) followed by addition of milli-Q water (at the ratio of 1:5) to give 1 mM stock solution. Oleanolic acid (OA) was dissolved in ethanol to attain 1 mM concentration. Artemisinin (ART) was dissolved in ethanol and mQ water (at a ratio 50:50) to attain 1 mM concentration.

Single-drug treatments.

Stock solutions were subjected to serial dilutions to give final concentrations ranging from 0.16 to 200 μM, using 10% RMPI 1640 medium. Cells at a density of 4000 to 6000 cells/well were treated with CS, OA and ART individually at four different concentrations, repeated three times in the same plate and incubated for 72 hours. Two controls were used; one contained cell and medium and the other contained (cells, medium and ethanol). Cytotoxic effects of CS, OA and ART alone at different concentrations were evaluated using MTT assay following the procedure described by Mosmann [137]. Briefly, after 72 h of incubation with drug(s), medium was replaced by adding fifty μL of MTT solution to each

 doi:10.20944/preprints202008.0667.v1

well followed by further 4 h incubation. Then one hundred fifty µL of DMSO was added to each well to dissolve formazan crystals after MTT solution was aspirated. The absorbance at 570 nm was measured using microplate reader [137]. Percentage of living cells was calculated by dividing the average of optical density of wells (containing treated cells) by the average of optical density of wells (containing untreated cells). Concentration of (CS, OA or ART) required to produce 50% of growth inhibition in each cell line compared to control (which is referred to as IC_{50} value) was obtained from the standard curve, representing the percentage of the cell viability versus the concentration.

Combination studies.

Cells were treated with solutions of compounds alone and in combination at three different concentrations, generally at constant ratios of their IC_{50} values. The concentration ranges were: cisplatin: 0.13-2.11 µM, 1.29- 20.61 µM and 1.67-26.78 µM; oleanolic acid: 6.80-108.80µM, 5.23-83.68 µM and 2.17-34.72 µM; artemisinin 3.36-53.70 mM, 5.36-85.76 mM and 7.27-116.35 mM for A2780 (parent), $A2780^{cisR}$ (cisplatin resistant) and $A2780^{ZD0473R}$ (ZD0473-resistant) cell lines respectively. Briefly, 100 µL of cells seeded in each well of 96-well plate were treated with CS, OA and ART alone and in combination with CS using the chosen concentrations, following three sequential modes; (Pt/ Phyt: 0,0 h), (Pt/ Phyt: 0/4 h) and (Pt/ Phyt: 4/0 h), non-treated cells served as control. The plates were incubated for 72 h with each experiment repeated three times. The inhibition of cell growth was determined using the (MTT) reduction assay as previously mentioned. The combination index (CI) value of two compounds in combination was determined according to the method

 doi:10.20944/preprints202008.0667.v1

developed by Chou and Talalay [14]. CI of <1, =1 and >1, indicates synergism, additiveness and antagonism respectively [14,138].

Platinum cellular accumulation and platinum–DNA binding studies.

A2780 and A2780^{cisR} cells with density of (5 x 10^6 mL^{-1}) in each petri dish treated with CS alone and its binary combinations with OA and ART using fixed concentrations of their IC_{50} values, were incubated for forty-eight hours. Cells were collected and centrifuged at 3500 rpm for two minutes at 4°C. Next, cell pellets were washed twice with 4 mL of cold PBS and centrifuged at 3500 rpm at 4°C for two minutes. Cell pellets were then re-suspended with 0.5 mL of cold PBS. Then (1.5 µL) was taken from each sample and mixed with the same quantity of tryphan blue to determine the cell survival fraction using the automated cell counter. The samples were then re-spun for two minutes at 10000 rpm at 4°C then cell pellets were stored at -20°C until assayed.

Cellular accumulation.

Cell pallets were lysed with 0.5 mL of 1% triton-X100 added to each sample and sonicated in ice for thirty minutes then centrifuged at 14000 rpm for three minutes. Then 400 µL of the supernatant from each sample was used to determine cellular platinum levels by measuring the absorbance values using graphite furnace AAS. The platinum level in each sample was calculated as nmol of platinum per 5x106 cells.

Platinum–DNA binding.

Cell pellet from each sample was re-suspended in 200 µL of PBS for DNA extraction using JETQUICK DNA Spin Kit following the protocol of the provider's instructions (see ref,

[139]. The DNA content was calculated from absorbance as A260 nm X 50 ng/µL [140]. A260/A280 ratio [140] between 1.75 and 1.8 for each sample ensured acceptable purity for tested samples. Next, 200 µL from each DNA sample was used for platinum level quantification using graphite furnace AAS.

Proteomic studies.

The proteomic studies were initially intended: 1) to determine the proteins that underwent changes in expression in A2780^{cisR} as compared to parent A2780 cell line and 2) to evaluate the effect of the selected combination treatments on those proteins. The studies were based on 2D-gel electrophoresis and the use of Melanie 7.0 software. The ultimate objective was to identify protein biomarkers that might be associated with the resistance towards CS, using MALDI TOF/TOF MS/MS. The identified spots were matched against Mascot (http://www.matrixscience.com), SwissProt database (http://www.uniprot.org/), at APAF (http://www.proteome.org.au/). *"This work was undertaken at APAF the infrastructure provided by the Australian Government through the National Collaborative Research Infrastructure Strategy (NCRIS)."*

Sample preparation, treatments, pellet collection and protein quantification:

A2780/ A2780^{cisR} (5×10^4) cells were seeded and incubated for 24 hours. The next day A2780^{cisR} cells were treated with chosen drug combinations namely (CS and ART using 4/0 h), (CS and OA using 0/4 h), (CS and ART using 0/0 h) and (CS and OA using 0/0 h), then all samples (including untreated samples from both cell lines) were incubated for 24 hours. Cells then were collected, centrifuged (at 3500 rpm, 2 min at 4ºC), washed (PBS/5 mL), re-suspend (by PBS/1 mL), counted, and centrifuged (at 14000 rpm, 2 min at 4°C).

Following this, the pellets were lysed in 500 µL of: (501 µL) of 65 mM DTT, (24.04 g) of 8 M Urea, (2.00 g) of 4 %CHAPS, (7.61 g) of 2 M thiourea, (5 tablets) protease inhibitor and (up to 50 mL) of mQ water. Subsequently, the pellets were lysed and centrifuged at (13, 000 rpm and 4ºC) for thirty minutes. Next, the supernatant was collected and stored at-80°C (see refs [141]. Total protein was measured as described by the assay kit provider [142], based on Bradford method [143]. The absorbance was measured at 595 nm using microplate reader BIO-RAD Model 3550. The standard curve was used to determine protein concentration of the samples.

Two-dimensional gel electrophoresis:

For protein separation, first-dimension IEF was performed following the technique of the provider's manual *[144] [1]. Briefly, the IPG strip (11 cm L× 3.3 mm W × 0.5 mm thick / 3-10 NL pH gradient) was passively rehydrated in 180 µL of rehydration solution containing: 4 % CHAPS 100 µL, 0.0002 % bromophenol blue, 60 mM DTT, 8 M Urea, (15mg/1mL) DeStreak, 2 M thiourea, and 0.2 % ampholytes with 200 µg of protein from each sample then the samples were kept overnight. Then IEF procedure was performed using PROTEAN i12 IEF system following the manufacturer's running protocol **[145]. The 2nd dimension was carried out using IPG strip, precast gels and criterion dodeca cell unit, following the procedures described in the product's instruction manual ***[146]. Briefly, IPG strips were incubated in (traces of bromophenol, 20% glycerol v/v, 2% DTT w/v, 50mM Tris– HCl pH 8.8, 2% SDS w/v, and 6 M urea) then were kept on a rocker for fifteen minutes **[145] Again,

[1] These Bio-Rad' manuals do not have author or published date, therefore, (*, ** and ***) was placed next to the reference to distinguish each instruction manual. However, the URL of each one is provided at the reference list. Also, they can be found at the company's website (https://www.bio-rad.com/) through their bulletin distinct numbers (bulletin #4110009, bulletin #2651 & bulletin #4006197).

the strips were incubated in (traces of bromophenol, 2% glycerol v/v, 50 mM Tris– HCl pH 8.8, 2% SDS w/v, 2% IAA w/v, and M urea) solution and left on a rocker for fifteen minutes **[145]. Next, IPG strips were washed with (192 mM glycine, 0.1% (w/v) SDS, pH 8.3, and 25 mM Tris). The Criterion Dodeca Cell was filled with 6 litres of (6 X) Tris/Glycine/SDS (0.1% SDS, 192 mM glycine, and 25 mM tris, pH (8.3). Before running the program, gel cassettes were sealed with a melted agarose **[145]. Sequentially, the unit was run for sixty-five minutes at 200V ***[146]. The gels were dyed with coomassie blue, scanned with the ChemiDoc XRS imaging system and saved as TIFF format (see, [147]. The paired gel images (12 gels, a duplicate for each gel sample) from untreated A2780 cell line, untreated A2780^{cisR} cell line, treated A2780^{cisR} cell with the following combinations: (CS and ART using 4/0 h), (CS and OA using 0/4 h) and (CS and ART using 0/0 h) and (CS and OA using 0/0 h), were imported into Melanie 7.0 software and clustered into six groups for spots detection and quantification, following the product's manual instructions (see, [148]. Briefly, the spot from the same sample was manually and automatically matched and paired using two landmarks. Next, the matched spots were annotated and assigned identical matched ID in all gel samples. Following this, the six groups were assembled into four hierarchical classes: 1) untreated A2780, 2) untreated A2780^{cisR}, 3) treated A2780^{cisR} with (CS and OA), and 4) treated A2780^{cisR} with (CS and ART), subsequently, spots were automatically analyzed and compared across all the samples using A2780 cell line as a reference after that untreated A2780^{cisR} cell line as reference then spots were quantified automatically. In this study, a two-fold or greater change in protein expression was considered significant. Based on this parameter, 101 spots out of 133 spots were selected and sent to APAF (Macquarie University)

for protein identification using MALDI-TOF and Mass Spectroscopy through APAF (http://www.proteome.org.au/). The detailed methods of MALDI and MS were previously described [149]. Briefly, at APAF (Macquarie University) (http://www.proteome.org.au/), using 4800 plus MALDI TOF/TOF Analyser (AB Sciex), spots were excised (spot cutter/ Bio-Rad), destained (ammonium bicarbonate / acetonitrile) and digested (ammonium bicarbonate, 16 h at 37ºC). Next, the peptides were extracted (0.1% TFA /C18 zip-tip) and yield (MALDI-MS). The most intense (8) peptide peaks (ions) from each spot were further fragmented by (CID system). Masses and intensities were measured by MS/MS (TOF-TOF) and matched against Mascot database (Matrix Science Ltd, London UK. (http://www.matrixscience.com/). Monoisotopic peak lists were matched against Homo sapiens using SwissProt database (http://www.uniprot.org/) [15]. The score was calculated according to Mascot parameter (http://www.matrixscience.com/) and as previously reported (greater than 56 is significant, $p<0.05$).

5. Conclusions

The results show that synergistic effect from combinations of CS with OA and ART in A2780, A2780^{cisR} and A2780^{ZD0473R} are dependent on the dose, time and cell type. The results show that the increased CS-DNA binding levels was consistent with the observed increase in CS-accumulation.. The results also show that platinum-DNA levels are greater in the A2780^{cisR} cells, indicating that the presence of ART and OA have modulated some of platinum resistance mechanisms, such as decreases of the platinum-DNA adducts formation [18], increases of platinum detoxification, and increases of DNA repair [19].

Investigation of proteins expression has shown that out of 101 proteins, (49) proteins were 2 ≥ fold differently expressed and were successfully identified by MS. Those proteins were shown to play a critical role in cell cycle regulation, pro-survival, and anti-survival pathways, suggesting their participation in platinum drug resistance. Most of the identified proteins are associated with molecular chaperones and stress, metabolism and invasion and metastasis. It can thus be suggested that those identified proteins can be additional novel predictive factors for early detection to individualised therapeutic interventions, considering the differences of each histologic type to improve the overall survival rate along with preserving the quality of the patient life. Finally, this study suggests that these synergistic combinations were able to restore back most of proteins' expressions in A2780^{cisR} cell line, thus, they can be deemed as valuable approaches to circumvent Pt-resistance associated with aberrant expression of those proteins in ovarian cancer. Based on this study, evaluations of cellular sensitivity/ resistance to those treatments *in vivo* studies using suitable animal models deserve to be further tested in the future. Studies on cellular DNA damage, oxidative stress and cell cycles may provide further mechanistic information.

Authors' contributions

SA developed the methodology, acquired and interpreted data, and drafted the manuscript. PB and JQY aided in study design. FH conceived and designed the study, developed the methodology, edited the manuscript, and oversaw the study. All authors have read and approved the final manuscript.

Competing interests

The authors declare no conflict of interest.

Supplementary Materials: Supplementary materials can be found at www.mdpi.com/xxx/s1.

Acknowledgments

Safiah Althurwi is grateful to Saudi Government for the award of a PhD scholarship. This research is partly supported by Biomedical Science Research Initiative Grant and Cancer Research Donation Fund. Part of the proteomic work was undertaken at APAF the Infrastructure provided by the Australian Government through the National Collaborative Research Infrastructure Strategy (NCRIS).

Abbreviations

$AgNO_3$: Silver nitrate; Akt: Serine threonine specific protein kinase; AP-1: Activator protein-1; APAF: Australian Proteome Analysis Facility; Bcl-XL: B-cell lymphoma-extra-large; CDK4: Cyclin-dependent kinase 4; CDKs: Cyclin-dependent protein Kinases; CHAPS: (3[3-Cholamidopropyl) dimethylammonio]-1-propanesulfonate); CI: Combination index; CNX: Lectin/chaperones calnexin; COX-2: Cyclooxygenase-2; CRT: Calreticulin cycle; DHAP: Dihydroxyacetone phosphate; Dm: The median-effect dose or concentration; DMSO: Dimethyl sulfoxide; DNA: Deoxyribonucleic Acid; DSB: DNA double strand breaks; DTT: Dithiothreitol; EGFR: Epidermal growth factor receptor; ESCC: Esophageal squamous cell carcinoma; FCS: Fetal calf serum; FoxM1: Fork head box protein M1; GAP: D-glyceraldehyde-3-phosphate; GBC-SD18H: Highly metastatic gallbladder carcinoma cells; HCC: Hepatocellular carcinoma; HGFR: Hepatocyte growth factor receptor; HIF1 α: Hypoxia-inducible factor 1 α; IAA: Iodoacetamide; IC^{50}: Inhibitory Concentration that causes 50% cell kill; $AgNO_3$: Silver nitrate; Akt: Serine threonine specific protein kinase; AP-1: Activator protein-1; APAF: Australian Proteome Analysis Facility; Bcl-XL: B-cell lymphoma-extra-large; CDK4: Cyclin-dependent kinase 4; CDKs: Cyclin-dependent protein Kinases; CHAPS: (3[3-Cholamidopropyl) dimethylammonio]-1-propanesulfonate); CI: Combination index; CNX: Lectin/chaperones calnexin; COX-2: Cyclooxygenase-2; CRT: Calreticulin cycle; DHAP: Dihydroxyacetone phosphate; Dm: The median-effect dose or concentration; DMSO: Dimethyl sulfoxide; DNA: Deoxyribonucleic Acid; DSB: DNA double strand breaks; DTT: Dithiothreitol; EGFR: Epidermal growth factor receptor; ESCC: Esophageal squamous cell carcinoma; FCS: Fetal calf serum; FoxM1: Fork head box protein M1; GAP: D-glyceraldehyde-3-phosphate; GBC-SD18H: Highly metastatic gallbladder carcinoma cells; HCC: Hepatocellular carcinoma; HGFR: Hepatocyte growth factor receptor; HIF1 α: Hypoxia-inducible factor 1 α; IAA: Iodoacetamide; IC^{50}: Inhibitory Concentration that causes 50% cell kill; IEF: Isoelectric focusing point; IPG: Immobiline pH gradient; ISC: Interstrand crosslinks; K2[PtCl4]: potassium tetrachloroplatinate (II); KCl: Potassium chloride; KI: potassium iodide;

 doi:10.20944/preprints202008.0667.v1

IEF: Isoelectric focusing point; IPG: Immobiline pH gradient; ISC: Interstrand crosslinks; K2[PtCl4]: potassium tetrachloroplatinate (II); KCl: Potassium chloride; KI: potassium iodide; MALDI -MS: Matrix Assisted Laser Desorption Ionisation mass spectrometry; MAPK: Mitogen-activated protein kinases; MCF-7: Breast cancer cells; MDR: Multiple drugs resistance; MMPs: Matrix metalloproteinase; mQ: Milli-Q water; MS: Mass Spectrometry; MTT: 3-(4, 5-dimethylthiazol -2-yl)-2, 5-diphenyltetrazolium bromide; NaHCO3: Sodium bicarbonate; NaOH: Sodium Hydroxide; NF-κB: Nuclear factor-kappa B; NKEF-A: Natural killer cell-enhancing factor A; p38: Mitogen-activated protein kinases; p53: Tumour suppressor protein; PAGE: polyacrylamide gel electrophoresis; PBS: Phosphate Buffered Saline; PDIs: Protein disulfide isomerases; Phyt: Phytochemical; pI: Isoelectric focusing point; PK: Pyruvate kinase; PKC: Protein kinase C; Pt: Platinum; R: The reliability coefficient; RAN: GTP-binding nuclear protein Ran; Ref-1 Redox effector factor 1; Ribonucleic acid; ROS: Reactive oxygen species; RPMI 1640: Roswell Park Memorial Institute 1640 media; SDS: sodium dodecyl sulfate; SDS-PAGE: Sodium dodecyl sulfate-polyacrylamide gel electrophoresis; TNF: Tumour necrosis factor; Triton-X 100:T-Octylphenooxypolyethoxyethanol; UPP: ubiquitin proteasome pathway; UPS: Ubiquitinated proteasomal system; UV: Ultraviolet: VEGF: Vascular endothelial growth factor; WNT2: Wnt family member 2; XIAP: X-linked inhibitor of apoptosis protein; ZD0473: Cis amminedichloro (2methylpyridine) platinum(II).

Cis amminedichloro (2methylpyridine) platinum(II).

Abbreviations

Abbreviations

Appendix A

The appendix is an optional section that can contain details and data supplemental to the main text. For example, explanations of experimental details that would disrupt the flow of the main text, but nonetheless remain crucial to understanding and reproducing the research shown; figures of replicates for experiments of which representative data is shown in the main text can be added here if brief, or as Supplementary data. Mathematical proofs of results not central to the paper can be added as an appendix.

Appendix B

All appendix sections must be cited in the main text. In the appendixes, Figures, Tables, etc. should be labeled starting with 'A', e.g., Figure A1, Figure A2, etc.

References

1. Nowak, M.; Glowacka, E.; Kielbik, M.; Kulig, A.; Sulowska, Z.; Klink, M. Secretion of cytokines and heat shock protein (HspA1A) by ovarian cancer cells depending on the tumor type and stage of disease. *Cytokine* **2017**, *89*, 136-142.
2. Hacker, N.F.; Rao, A. Surgery for advanced epithelial ovarian cancer. *Best Practice & Research Clinical Obstetrics & Gynaecology* **2017**, *41*, 71-87.
3. Aletti, G.D.; Peiretti, M. Quality control in ovarian cancer surgery. *Best Practice & Research Clinical Obstetrics & Gynaecology* **2017**, *41*, 96-107.
4. Florea, A.-M.; Büsselberg, D. Cisplatin as an anti-tumor drug: cellular mechanisms of activity, drug resistance and induced side effects. *Cancers (Basel)* **2011**, *3*, 1351-1371.
5. Sarkar, F.H.; Li, Y. Using chemopreventive agents to enhance the efficacy of cancer therapy. *Cancer Res.* **2006**, *66*, 3347-3350.
6. Amable, L. Cisplatin resistance and opportunities for precision medicine. *Pharmacol. Res.* **2016**, *106*, 27-36, doi:10.1016/j.phrs.2016.01.001.
7. Ohmichi, M.; Hayakawa, J.; Tasaka, K.; Kurachi, H.; Murata, Y. Mechanisms of platinum drug resistance. *Trends Pharmacol. Sci.* **2005**, *26*, 113-116.
8. Apps, M.G.; Choi, E.H.; Wheate, N.J. The state-of-play and future of platinum drugs. *Endocr. Relat. Cancer* **2015**, *22*, R219-R233.
9. Pollier, J.; Goossens, A. Oleanolic acid. *Phytochemistry* **2012**, *77*, 10-15, doi:http://dx.doi.org/10.1016/j.phytochem.2011.12.022.
10. Žiberna, L.; Šamec, D.; Mocan, A.; Nabavi, S.F.; Bishayee, A.; Farooqi, A.A.; Sureda, A.; Nabavi, S.M. Oleanolic Acid Alters Multiple Cell Signaling Pathways: Implication in Cancer Prevention and Therapy. *Int. J. Mol. Sci.* **2017**, *18*, 643.
11. Zhang, R.-W. Artemisinin (Qinghaosu), Nobel Prize, anti-malaria, and beyond. *Chinese Journal of Natural Medicines* **2016**, *14*, 1-2, doi:http://dx.doi.org/10.3724/SP.J.1009.2016.00001.
12. Weathers, P.J.; Cambra, H.M.; Desrosiers, M.R.; Rassias, D.; Towler, M.J. Chapter 5 - Artemisinin the Nobel Molecule: From Plant to Patient. In *Studies in Natural Products Chemistry*, Atta ur, R., Ed. Elsevier: 2017; Vol. 52, pp. 193-229.

13. Gong, X.-m.; Zhang, Q.; Torossian, A.; Cao, J.-p.; Fu, S. Selective radiosensitization of human cervical cancer cells and normal cells by artemisinin through the abrogation of radiation-induced G2 block. *Int. J. Gynecol. Cancer* **2012**, *22*, 718-724.
14. Chou, T.-C.; Talalay, P. Quantitative analysis of dose-effect relationships: the combined effects of multiple drugs or enzyme inhibitors. *Adv. Enzyme Regul.* **1984**, *22*, 27-55, doi:https://doi.org/10.1016/0065-2571(84)90007-4.
15. UniPortKB. Protein Knowledgebase. Availabe online: http://www.uniprot.org/uniprot/ (accessed on 28 December).
16. Shanmugam, M.K.; Lee, J.H.; Chai, E.Z.P.; Kanchi, M.M.; Kar, S.; Arfuso, F.; Dharmarajan, A.; Kumar, A.P.; Ramar, P.S.; Looi, C.Y., et al. Cancer prevention and therapy through the modulation of transcription factors by bioactive natural compounds. *Semin. Cancer Biol.* **2016**, *40-41*, 35-47, doi:https://doi.org/10.1016/j.semcancer.2016.03.005.
17. Firestone, G.L.; Sundar, S.N. Anticancer activities of artemisinin and its bioactive derivatives. *Expert Rev. Mol. Med.* **2009**, *11*, e32.
18. Dasari, S.; Tchounwou, P.B. Cisplatin in cancer therapy: molecular mechanisms of action. *Eur. J. Pharmacol.* **2014**, *740*, 364-378.
19. Wexselblatt, E.; Yavin, E.; Gibson, D. Cellular interactions of platinum drugs. *Inorganica Chimica Acta* **2012**, *393*, 75-83.
20. Song, I.-S.; Savaraj, N.; Siddik, Z.H.; Liu, P.; Wei, Y.; Wu, C.J.; Kuo, M.T. Role of human copper transporter Ctr1 in the transport of platinum-based antitumor agents in cisplatin-sensitive and cisplatin-resistant cells. *Mol. Cancer Ther.* **2004**, *3*, 1543-1549.
21. Mazumder, M.E.H.; Beale, P.; Chan, C.; Yu, J.Q.; Huq, F. Studies on New Tumour Active Palladium Complexes Targeted to Overcome Resistance in Ovarian Cancer. University of Sydney, ,Australia, 2013.
22. Gamberi, T.; Massai, L.; Magherini, F.; Landini, I.; Fiaschi, T.; Scaletti, F.; Gabbiani, C.; Bianchi, L.; Bini, L.; Nobili, S., et al. Proteomic analysis of A2780/S ovarian cancer cell response to the cytotoxic organogold(III) compound Aubipyc. *J. Proteomics* **2014**, *103*, 103-120, doi:https://doi.org/10.1016/j.jprot.2014.03.032.
23. Liu, F.-t.; Chen, Y.; Yang, Y.-j.; Yang, L.; Yu, M.; Zhao, J.; Wu, J.-j.; Huang, F.; Liu, W.; Ding, Z.-t. Involvement of mortalin/GRP75/mthsp70 in the mitochondrial impairments induced by A53T mutant α-synuclein. *Brain Res.* **2015**, *1604*, 52-61.
24. Yang, L.; Li, H.; Jiang, Y.; Zuo, J.; Liu, W. Inhibition of mortalin expression reverses cisplatin resistance and attenuates growth of ovarian cancer cells. *Cancer Lett.* **2013**, *336*, 213-221.
25. Nessa, M.U.; Beale, P.; Chan, C.; Yu, J.Q.; Huq, F. Studies on Combinations Between Platinum Drugs and Phytochemicals in Ovarian Tumour Models. University of Sydney, ,Australia, 2013.
26. Al-Eisawi, Z.; Beale, P.; Chan, C.; Yu, J.Q.; Huq, F. Combinations between platinum drugs and bortezomib and changes in nature of administration in ovarian tumour models. University of Sydney, ,Australia, 2013.
27. Alamro, A.A.S.; Beale, P.; Chan, C.; Yu, J.Q.; Huq, F. Studies on combination between tumour active compounds in ovarian tumour models. University of Sydney, ,Australia, 2015.
28. Li, Y.; Chen, X.; Shi, M.; Wang, H.; Cao, W.; Wang, X.; Li, C.; Feng, W. Proteomic-based identification of Apg-2 as a therapeutic target for chronic myeloid leukemia. *Cell. Signal.* **2013**, *25*, 2604-2612.

29. Kang, J.; Zhao, G.; Lin, T.; Tang, S.; Xu, G.; Hu, S.; Bi, Q.; Guo, C.; Sun, L.; Han, S. A peptide derived from phage display library exhibits anti-tumor activity by targeting GRP78 in gastric cancer multidrug resistance cells. *Cancer Lett.* **2013**, *339*, 247-259.
30. Lee, A.S. GRP78 induction in cancer: therapeutic and prognostic implications. *Cancer Res.* **2007**, *67*, 3496-3499.
31. Yang, L.; Yang, S.; Liu, J.; Wang, X.; Ji, J.; Cao, Y.; Lu, K.; Wang, J.; Gao, Y. Expression of GRP78 predicts taxane-based therapeutic resistance and recurrence of human gastric cancer. *Exp. Mol. Pathol.* **2014**, *96*, 235-241.
32. Lauber, K.; Brix, N.; Ernst, A.; Hennel, R.; Krombach, J.; Anders, H.; Belka, C. Targeting the heat shock response in combination with radiotherapy: Sensitizing cancer cells to irradiation-induced cell death and heating up their immunogenicity. *Cancer Lett.* **2015**, *368*, 209-229.
33. Partridge, J.R.; Lavery, L.A.; Elnatan, D.; Naber, N.; Cooke, R.; Agard, D.A. A novel N-terminal extension in mitochondrial TRAP1 serves as a thermal regulator of chaperone activity. *eLife* **2015**, *3*, e03487.
34. Subbarao Sreedhar, A.; Kalmár, É.; Csermely, P.; Shen, Y.-F. Hsp90 isoforms: functions, expression and clinical importance. *Federation of European Biochemical Societies Letters* **2004**, *562*, 11-15.
35. Elstrand, M.B.; Stavnes, H.T.; Tropé, C.G.; Davidson, B. Heat shock protein 90 is a putative therapeutic target in patients with recurrent advanced-stage ovarian carcinoma with serous effusions. *Hum. Pathol.* **2012**, *43*, 529-535.
36. Dejeans, N.; Glorieux, C.; Guenin, S.; Beck, R.; Sid, B.; Rousseau, R.; Bisig, B.; Delvenne, P.; Calderon, P.B.; Verrax, J. Overexpression of GRP94 in breast cancer cells resistant to oxidative stress promotes high levels of cancer cell proliferation and migration: implications for tumor recurrence. *Free Radic. Biol. Med.* **2012**, *52*, 993-1002.
37. Lou, J.; Fatima, N.; Xiao, Z.; Stauffer, S.; Smythers, G.; Greenwald, P.; Ali, I.U. Proteomic profiling identifies cyclooxygenase-2-independent global proteomic changes by celecoxib in colorectal cancer cells. *Cancer Epidemiology and Prevention Biomarkers* **2006**, *15*, 1598-1606.
38. Lee, J.; Kim, S.S. Current implications of cyclophilins in human cancers. *J. Exp. Clin. Cancer Res.* **2010**, *29*, 1.
39. Nath, P.R.; Isakov, N. Insights into peptidyl-prolyl cis–trans isomerase structure and function in immunocytes. *Immunol. Lett.* **2015**, *163*, 120-131, doi:http://dx.doi.org/10.1016/j.imlet.2014.11.002.
40. Pinto, R.D.; Moreira, A.R.; Pereira, P.J.; dos Santos, N.M. Two thioredoxin-superfamily members from sea bass (Dicentrarchus labrax, L.): Characterization of PDI (PDIA1) and ERp57 (PDIA3). *Fish Shellfish Immunol.* **2013**, *35*, 1163-1175.
41. Kullmann, M.; Kalayda, G.V.; Hellwig, M.; Kotz, S.; Hilger, R.A.; Metzger, S.; Jaehde, U. Assessing the contribution of the two protein disulfide isomerases PDIA1 and PDIA3 to cisplatin resistance. *J. Inorg. Biochem.* **2015**, *153*, 247-252.
42. Caorsi, C.; Niccolai, E.; Capello, M.; Vallone, R.; Chattaragada, M.S.; Alushi, B.; Castiglione, A.; Ciccone, G.; Mautino, A.; Cassoni, P. Protein disulfide isomerase A3–specific Th1 effector cells infiltrate colon cancer tissue of patients with circulating anti–protein disulfide isomerase A3 autoantibodies. *Translational Research* **2016**, *171*, 17-28. e12.

43. Andreu, C.I.; Woehlbier, U.; Torres, M.; Hetz, C. Protein disulfide isomerases in neurodegeneration: from disease mechanisms to biomedical applications. *Federation of European Biochemical Societies Letters* **2012**, *586*, 2826-2834.
44. Trnková, L.; Ricci, D.; Grillo, C.; Colotti, G.; Altieri, F. Green tea catechins can bind and modify ERp57/PDIA3 activity. *Biochimica et Biophysica Acta (BBA)-General Subjects* **2013**, *1830*, 2671-2682.
45. Lee, E.; Lee, D.H. Emerging roles of protein disulfide isomerase in cancer. *BMB reports* **2017**, *50*, 401.
46. Leys, C.M.; Nomura, S.; LaFleur, B.J.; Ferrone, S.; Kaminishi, M.; Montgomery, E.; Goldenring, J.R. Expression and prognostic significance of prothymosin-α and ERp57 in human gastric cancer. *Surgery* **2007**, *141*, 41-50, doi:http://dx.doi.org/10.1016/j.surg.2006.05.009.
47. Ren, F.; Wu, H.; Lei, Y.; Zhang, H.; Liu, R.; Zhao, Y.; Chen, X.; Zeng, D.; Tong, A.; Chen, L. Quantitative proteomics identification of phosphoglycerate mutase 1 as a novel therapeutic target in hepatocellular carcinoma. *Mol. Cancer* **2010**, *9*, 81.
48. Zha, X.; Wang, F.; Wang, Y.; He, S.; Jing, Y.; Wu, X.; Zhang, H. Lactate dehydrogenase B is critical for hyperactive mTOR-mediated tumorigenesis. *Cancer Res.* **2011**, *71*, 13-18.
49. Huang, S.K.; Darfler, M.M.; Nicholl, M.B.; You, J.; Bemis, K.G.; Tegeler, T.J.; Wang, M.; Wery, J.-P.; Chong, K.K.; Nguyen, L. LC/MS-based quantitative proteomic analysis of paraffin-embedded archival melanomas reveals potential proteomic biomarkers associated with metastasis. *Public Library of Science one* **2009**, *4*, e4430.
50. Chang, Y.-H.; Wu, C.-C.; Chang, K.-P.; Yu, J.-S.; Chang, Y.-C.; Liao, P.-C. Cell secretome analysis using hollow fiber culture system leads to the discovery of CLIC1 protein as a novel plasma marker for nasopharyngeal carcinoma. *J. Proteome Res.* **2009**, *8*, 5465-5474.
51. Ding, S.J.; Li, Y.; Shao, X.X.; Zhou, H.; Zeng, R.; Tang, Z.Y.; Xia, Q.C. Proteome analysis of hepatocellular carcinoma cell strains, MHCC97-H and MHCC97-L, with different metastasis potentials. *Proteomics* **2004**, *4*, 982-994.
52. Wang, J.-W.; Peng, S.-Y.; Li, J.-T.; Wang, Y.; Zhang, Z.-P.; Cheng, Y.; Cheng, D.-Q.; Weng, W.-H.; Wu, X.-S.; Fei, X.-Z. Identification of metastasis-associated proteins involved in gallbladder carcinoma metastasis by proteomic analysis and functional exploration of chloride intracellular channel 1. *Cancer Lett.* **2009**, *281*, 71-81.
53. Lamb, R.; Harrison, H.; Hulit, J.; Smith, D.L.; Lisanti, M.P.; Sotgia, F. Mitochondria as new therapeutic targets for eradicating cancer stem cells: Quantitative proteomics and functional validation via MCT1/2 inhibition. *Oncotarget* **2014**, *5*, 11029-11037.
54. Onda, M.; Emi, M.; Yoshida, A.; Miyamoto, S.; Akaishi, J.; Asaka, S.; Mizutani, K.; Shimizu, K.; Nagahama, M.; Ito, K. Comprehensive gene expression profiling of anaplastic thyroid cancers with cDNA microarray of 25 344 genes. *Endocr. Relat. Cancer* **2004**, *11*, 843-854.
55. Duffy, M.J. Predictive markers in breast and other cancers: a review. *Clin. Chem.* **2005**, *51*, 494-503.
56. Wang, J.; Tai, L.-S.; Tzang, C.-H.; Fong, W.F.; Guan, X.-Y.; Yang, M. 1p31, 7q21 and 18q21 chromosomal aberrations and candidate genes in acquired vinblastine resistance of human cervical carcinoma KB cells. *Oncol. Rep.* **2008**, *19*, 1155-1164.
57. Hofmann, W.-K.; de Vos, S.; Elashoff, D.; Gschaidmeier, H.; Hoelzer, D.; Koeffler, H.P.; Ottmann, O.G. Relation between resistance of Philadelphia-chromosome-positive acute lymphoblastic leukaemia to the tyrosine kinase inhibitor STI571 and gene-expression profiles: a gene-expression study. *The Lancet* **2002**, *359*, 481-486.

58. Soltysova, A.; Breza, J.; Takacova, M.; Feruszova, J.; Hudecova, S.; Novotna, B.; Rozborilova, E.; Pastorekova, S.; Kadasi, L.; Krizanova, O. Deregulation of energetic metabolism in the clear cell renal cell carcinoma: A multiple pathway analysis based on microarray profiling. *Int. J. Oncol.* **2015**, *47*, 287-295.
59. Yusenko, M.V.; Ruppert, T.; Kovacs, G. Analysis of differentially expressed mitochondrial proteins in chromophobe renal cell carcinomas and renal oncocytomas by 2-D gel electrophoresis. *Int. J. Biol. Sci.* **2010**, *6*, 213-224.
60. Chen, G.; Gharib, T.G.; Huang, C.-C.; Thomas, D.G.; Shedden, K.A.; Taylor, J.M.; Kardia, S.L.; Misek, D.E.; Giordano, T.J.; Iannettoni, M.D. Proteomic analysis of lung adenocarcinoma identification of a highly expressed set of proteins in tumors. *Clin. Cancer Res.* **2002**, *8*, 2298-2305.
61. Zhang, X.z.; Xiao, Z.f.; Li, C.; Xiao, Z.q.; Yang, F.; Li, D.j.; Li, M.y.; Li, F.; Chen, Z.c. Triosephosphate isomerase and peroxiredoxin 6, two novel serum markers for human lung squamous cell carcinoma. *Cancer Sci.* **2009**, *100*, 2396-2401.
62. Altenberg, B.a.; Greulich, K. Genes of glycolysis are ubiquitously overexpressed in 24 cancer classes. *Genomics* **2004**, *84*, 1014-1020.
63. Di Michele, M.; Marcone, S.; Cicchillitti, L.; Della Corte, A.; Ferlini, C.; Scambia, G.; Donati, M.B.; Rotilio, D. Glycoproteomics of paclitaxel resistance in human epithelial ovarian cancer cell lines: towards the identification of putative biomarkers. *J. Proteomics* **2010**, *73*, 879-898.
64. Jiang, X.; Chang, H.; Zhou, Y. Expression, purification and preliminary crystallographic studies of human glutamate oxaloacetate transaminase 1 (GOT1). *Protein Expr. Purif.* **2015**, *113*, 102-106.
65. Yu, M.; Zhou, Q.; Zhou, Y.; Fu, Z.; Tan, L.; Ye, X.; Zeng, B.; Gao, W.; Zhou, J.; Liu, Y. Metabolic phenotypes in pancreatic cancer. *Public Library of Science one* **2015**, *10*, e0115153.
66. Chakrabarti, G. Mutant KRAS associated malic enzyme 1 expression is a predictive marker for radiation therapy response in non-small cell lung cancer. *Radiation Oncology* **2015**, *10*, 145.
67. Takács-Vellai, K. The metastasis suppressor Nm23 as a modulator of Ras/ERK signaling. *J. Mol. Signal.* **2014**, *9*, 4.
68. Jin, L.; Liu, G.; Zhang, C.-h.; Lu, C.-h.; Xiong, S.; Zhang, M.-Y.; Liu, Q.-Y.; Ge, F.; He, Q.-Y.; Kitazato, K., et al. Nm23-H1 regulates the proliferation and differentiation of the human chronic myeloid leukemia K562 cell line: A functional proteomics study. *Life Sci.* **2009**, *84*, 458-467, doi:http://dx.doi.org/10.1016/j.lfs.2009.01.010.
69. Yi, S.; Guangqi, H.; Guoli, H. The association of the expression of MTA1, nm23H1 with the invasion, metastasis of ovarian carcinoma. *Chin. Med. Sci. J.* **2003**, *18*, 87-92.
70. Liu, S.; Sun, Y.; Tian, D.; He, Y.; Zeng, L.; He, Y.; Ling, C.; Sun, S. Downregulated NM23-H1 expression is associated with intracranial invasion of nasopharyngeal carcinoma. *Br. J. Cancer* **2008**, *98*, 363-369.
71. Yang, R.-F.; Sun, L.-H.; Zhang, R.; Zhang, Y.; Luo, Y.-X.; Zheng, W.; Zhang, Z.-Q.; Chen, H.-Z.; Liu, D.-P. Suppression of Mic60 compromises mitochondrial transcription and oxidative phosphorylation. *Sci. Rep.* **2015**, *5*, 7990, doi:10.1038/srep07990.
72. Liu, Z.; Marquez, M.; Nilsson, S.; Holmberg, A.R. Comparison of protein expression in two prostate cancer cell-lines, LNCaP and DU145, after treatment with somatostatin. *Oncol. Rep.* **2009**, *22*, 1451-1458.

73. Wong, T.S.; Liu, X.B.; Chung-Wai Ho, A.; Po-Wing Yuen, A.; Wai-Man Ng, R.; Ignace Wei, W. Identification of pyruvate kinase type M2 as potential oncoprotein in squamous cell carcinoma of tongue through microRNA profiling. *Int. J. Cancer* **2008**, *123*, 251-257.

74. He, Y.; Wang, Y.; Liu, H.; Xu, X.; He, S.; Tang, J.; Huang, Y.; Miao, X.; Wu, Y.; Wang, Q. Pyruvate kinase isoform M2 (PKM2) participates in multiple myeloma cell proliferation, adhesion and chemoresistance. *Leuk. Res.* **2015**, *39*, 1428-1436.

75. Sun, Q.; Chen, X.; Ma, J.; Peng, H.; Wang, F.; Zha, X.; Wang, Y.; Jing, Y.; Yang, H.; Chen, R. Mammalian target of rapamycin up-regulation of pyruvate kinase isoenzyme type M2 is critical for aerobic glycolysis and tumor growth. *Proceedings of the National Academy of Sciences* **2011**, *108*, 4129-4134.

76. Li, X.-H.; Li, C.; Xiao, Z.-Q. Proteomics for identifying mechanisms and biomarkers of drug resistance in cancer. *J. Proteomics* **2011**, *74*, 2642-2649.

77. Martinez-Balibrea, E.; Plasencia, C.; Ginés, A.; Martinez-Cardús, A.; Musulén, E.; Aguilera, R.; Manzano, J.L.; Neamati, N.; Abad, A. A proteomic approach links decreased pyruvate kinase M2 expression to oxaliplatin resistance in patients with colorectal cancer and in human cell lines. *Mol. Cancer Ther.* **2009**, *8*, 771-778.

78. Desai, S.; Ding, M.; Wang, B.; Lu, Z.; Zhao, Q.; Shaw, K.; Yung, W.; Weinstein, J.N.; Tan, M.; Yao, J. Tissue-specific isoform switch and DNA hypomethylation of the pyruvate kinase PKM gene in human cancers. *Oncotarget* **2014**, *5*, 8202-8210.

79. Baek, J.Y.; JUN, D.Y.; Dennis, T.; Kim, Y.H. Characterization of human phosphoserine aminotransferase involved in the phosphorylated pathway of L-serine biosynthesis. *Biochem. J.* **2003**, *373*, 191-200.

80. Vié, N.; Copois, V.; Bascoul-Mollevi, C.; Denis, V.; Bec, N.; Robert, B.; Fraslon, C.; Conseiller, E.; Molina, F.; Larroque, C. Overexpression of phosphoserine aminotransferase PSAT1 stimulates cell growth and increases chemoresistance of colon cancer cells. *Mol. Cancer* **2008**, ***7***, 14.

81. Toyama, A.; Suzuki, A.; Shimada, T.; Aoki, C.; Aoki, Y.; Umino, Y.; Nakamura, Y.; Aoki, D.; Sato, T.A. Proteomic characterization of ovarian cancers identifying annexin-A4, phosphoserine aminotransferase, cellular retinoic acid-binding protein 2, and serpin B5 as histology-specific biomarkers. *Cancer Sci.* **2012**, *103*, 747-755.

82. Arif, T.; Krelin, Y.; Shoshan-Barmatz, V. Reducing VDAC1 expression induces a non-apoptotic role for pro-apoptotic proteins in cancer cell differentiation. *Biochimica et Biophysica Acta (BBA)-Bioenergetics* **2016**, *1857*, 1228-1242.

83. Shoshan-Barmatz, V.; Ben-Hail, D.; Admoni, L.; Krelin, Y.; Tripathi, S.S. The mitochondrial voltage-dependent anion channel 1 in tumor cells. *Biochimica et Biophysica Acta (BBA)-Biomembranes* **2015**, *1848*, 2547-2575.

84. Capello, M.; Ferri-Borgogno, S.; Cappello, P.; Novelli, F. alpha-Enolase: a promising therapeutic and diagnostic tumor target. *Federation of European Biochemical Societies Journal* **2011**, *278*, 1064-1074, doi:10.1111/j.1742-4658.2011.08025.x.

85. Capello, M.; Caorsi, C.; Bogantes Hernandez, P.J.; Dametto, E.; Bertinetto, F.E.; Magistroni, P.; Rendine, S.; Amoroso, A.; Novelli, F. Phosphorylated alpha-enolase induces autoantibodies in HLA-DR8 pancreatic cancer patients and triggers HLA-DR8 restricted T-cell activation. *Immunol. Lett.* **2015**, *167*, 11-16, doi:http://dx.doi.org/10.1016/j.imlet.2015.06.008.

86. Satelli, A.; Li, S. Vimentin in cancer and its potential as a molecular target for cancer therapy. *Cell. Mol. Life Sci.* **2011**, *68*, 3033-3046.

87. Kidd, M.E.; Shumaker, D.K.; Ridge, K.M. The role of vimentin intermediate filaments in the progression of lung cancer. *Am. J. Respir. Cell Mol. Biol.* **2014**, *50*, 1-6, doi:10.1165/rcmb.2013-0314TR.

88. Fontana, S.; Alessandro, R.; Barranca, M.; Giordano, M.; Corrado, C.; Zanella-Cleon, I.; Becchi, M.; Kohn, E.C.; De Leo, G. Comparative proteome profiling and functional analysis of chronic myelogenous leukemia cell lines. *J. Proteome Res.* **2007**, *6*, 4330-4342.

89. Chiang, W.-L.; Chu, S.-C.; Yang, S.-S.; Li, M.-C.; Lai, J.-C.; Yang, S.-F.; Chiou, H.-L.; Hsieh, Y.-S. The aberrant expression of cytosolic carbonic anhydrase and its clinical significance in human non-small cell lung cancer. *Cancer Lett.* **2002**, *188*, 199-205.

90. Kuo, W.-H.; Chiang, W.-L.; Yang, S.-F.; Yeh, K.-T.; Yeh, C.-M.; Hsieh, Y.-S.; Chu, S.-C. The differential expression of cytosolic carbonic anhydrase in human hepatocellular carcinoma. *Life Sci.* **2003**, *73*, 2211-2223.

91. Goldmann, W.H.; Auernheimer, V.; Thievessen, I.; Fabry, B. Vinculin, cell mechanics and tumour cell invasion. *Cell Biol. Int.* **2013**, *37*, 397-405.

92. Cao, X.X.; Xu, J.D.; Liu, X.L.; Xu, J.W.; Wang, W.J.; Li, Q.Q.; Chen, Q.; Xu, Z.D.; Liu, X.P. RACK1: A superior independent predictor for poor clinical outcome in breast cancer. *Int. J. Cancer* **2010**, *127*, 1172-1179.

93. Shi, S.; Deng, Y.-Z.; Zhao, J.-S.; Ji, X.-D.; Shi, J.; Feng, Y.-X.; Li, G.; Li, J.-J.; Zhu, D.; Koeffler, H.P. RACK1 promotes non-small-cell lung cancer tumorigenicity through activating sonic hedgehog signaling pathway. *J. Biol. Chem.* **2012**, *287*, 7845-7858.

94. Kuramitsu, Y.; Wang, Y.; Okada, F.; Baron, B.; Tokuda, K.; Kitagawa, T.; Akada, J.; Nakamura, K. Malignant progressive tumor cell clone exhibits significant up-regulation of cofilin-2 and 27-kDa modified form of cofilin-1 compared to regressive clone. *Anticancer Res.* **2013**, *33*, 3661-3665.

95. Yan, H.; Yang, K.; Xiao, H.; Zou, Y.-J.; Zhang, W.-B.; Liu, H.-Y. Over-expression of cofilin-1 and phosphoglycerate kinase 1 in astrocytomas involved in pathogenesis of radioresistance. *CNS Neurosci. Ther.* **2012**, *18*, 729-736, doi:10.1111/j.1755-5949.2012.00353.x.

96. Tariq, M.; Ito, A.; Ishfaq, M.; Bradshaw, E.; Yoshida, M. Eukaryotic translation initiation factor 5A (eIF5A) is essential for HIF-1α activation in hypoxia. *Biochem. Biophys. Res. Commun.* **2016**, *470*, 417-424.

97. Mathews, M.B.; Hershey, J.W. The translation factor eIF5A and human cancer. *Biochimica et Biophysica Acta (BBA)-Gene Regulatory Mechanisms* **2015**, *1849*, 836-844.

98. Scuoppo, C.; Miething, C.; Lindqvist, L.; Reyes, J.; Ruse, C.; Appelmann, I.; Yoon, S.; Krasnitz, A.; Teruya-Feldstein, J.; Pappin, D. A tumour suppressor network relying on the polyamine-hypusine axis. *Nature* **2012**, *487*, 244-248.

99. Nakamura, J.; Aoyagi, S.; Nanchi, I.; Nakatsuka, S.-I.; Hirata, E.; Shibata, S.; Fukuda, M.; Yamamoto, Y.; Fukuda, I.; Tatsumi, N. Overexpression of eukaryotic elongation factor eEF2 in gastrointestinal cancers and its involvement in G2/M progression in the cell cycle. *Int. J. Oncol.* **2009**, *34*, 1181.

100. Hamrita, B.; Nasr, H.B.; Hammann, P.; Kuhn, L.; Guillier, C.-L.; Chaieb, A.; Khairi, H.; Chahed, K. An elongation factor-like protein (EF-Tu) elicits a humoral response in infiltrating ductal breast carcinomas: an immunoproteomics investigation. *Clin. Biochem.* **2011**, *44*, 1097-1104.

101. Tomaino, B.; Cappello, P.; Capello, M.; Fredolini, C.; Ponzetto, A.; Novarino, A.; Ciuffreda, L.; Bertetto, O.; De Angelis, C.; Gaia, E. Autoantibody signature in human ductal pancreatic adenocarcinoma. *J. Proteome Res.* **2007**, *6*, 4025-4031.

102. Srisomsap, C.; Sawangareetrakul, P.; Subhasitanont, P.; Panichakul, T.; Keeratichamroen, S.; Lirdprapamongkol, K.; Chokchaichamnankit, D.; Sirisinha, S.; Svasti, J. Proteomic analysis of cholangiocarcinoma cell line. *Proteomics* **2004**, *4*, 1135-1144.

103. Sen, S.; Ateeq, B.; Sharma, H.; Datta, P.; Gupta, S.D.; Bal, S.; Kumar, A.; Singh, N. Molecular profiling of genes in squamous cell lung carcinoma in Asian Indians. *Life Sci.* **2008**, *82*, 772-779.

104. Ryningen, A.; Ersvær, E.; Øyan, A.M.; Kalland, K.-H.; Vintermyr, O.K.; Gjertsen, B.T.; Bruserud, Ø. Stress-induced in vitro apoptosis of native human acute myelogenous leukemia (AML) cells shows a wide variation between patients and is associated with low BCL-2: Bax ratio and low levels of heat shock protein 70 and 90. *Leuk. Res.* **2006**, *30*, 1531-1540.

105. Ogawa, K.; Utsunomiya, T.; Mimori, K.; Tanaka, Y.; Tanaka, F.; Inoue, H.; Murayama, S.; Mori, M. Clinical significance of elongation factor-1 delta mRNA expression in oesophageal carcinoma. *Br. J. Cancer* **2004**, *91*, 282-286.

106. Chen, R.; Eugene, C.Y.; Donohoe, S.; Pan, S.; Eng, J.; Cooke, K.; Crispin, D.A.; Lane, Z.; Goodlett, D.R.; Bronner, M.P. Pancreatic cancer proteome: the proteins that underlie invasion, metastasis, and immunologic escape. *Gastroenterology* **2005**, *129*, 1187-1197.

107. Zhong, D.; Zhang, J.; Yang, S.; Soh, U.J.; Buschdorf, J.P.; Zhou, Y.T.; Yang, D.; Low, B.C. The SAM domain of the RhoGAP DLC1 binds EF1A1 to regulate cell migration. *J. Cell Sci.* **2009**, *122*, 414-424.

108. Carpenter, B.; MacKay, C.; Alnabulsi, A.; MacKay, M.; Telfer, C.; Melvin, W.T.; Murray, G.I. The roles of heterogeneous nuclear ribonucleoproteins in tumour development and progression. *Biochimica et Biophysica Acta (BBA)-Reviews on Cancer* **2006**, *1765*, 85-100.

109. Jean-Philippe, J.; Paz, S.; Caputi, M. hnRNP A1: the Swiss army knife of gene expression. *Int. J. Mol. Sci.* **2013**, *14*, 18999-19024.

110. Pino, I.; Pio, R.; Toledo, G.; Zabalegui, N.; Vicent, S.; Rey, N.; Lozano, M.D.; Torre, W.; Garcia-Foncillas, J.; Montuenga, L.M. Altered patterns of expression of members of the heterogeneous nuclear ribonucleoprotein (hnRNP) family in lung cancer. *Lung Cancer* **2003**, *41*, 131-143.

111. Chen, Z.-Y.; Cai, L.; Zhu, J.; Chen, M.; Chen, J.; Li, Z.-H.; Liu, X.-D.; Wang, S.-G.; Bie, P.; Jiang, P. Fyn requires HnRNPA2B1 and Sam68 to synergistically regulate apoptosis in pancreatic cancer. *Carcinogenesis* **2011**, *32*, 1419-1426.

112. Yan-Sanders, Y.; Hammons, G.J.; Lyn-Cook, B.D. Increased expression of heterogeneous nuclear ribonucleoprotein A2/B1 (hnRNP) in pancreatic tissue from smokers and pancreatic tumor cells. *Cancer Lett.* **2002**, *183*, 215-220.

113. Zhang, D.; Tai, L.K.; Wong, L.L.; Chiu, L.-L.; Sethi, S.K.; Koay, E.S. Proteomic study reveals that proteins involved in metabolic and detoxification pathways are highly expressed in her-2/neu-positive breast cancer*. *Mol. Cell. Proteomics* **2005**, *4*, 1686-1696.

114. Duan, Z.; Lamendola, D.; Yusuf, R.; Penson, R.; Preffer, F.; Seiden, M. Overexpression of human phosphoglycerate kinase 1 (PGK1) induces a multidrug resistance phenotype. *Anticancer Res.* **2001**, *22*, 1933-1941.

115. Hwang, T.L.; Liang, Y.; Chien, K.Y.; Yu, J.S. Overexpression and elevated serum levels of phosphoglycerate kinase 1 in pancreatic ductal adenocarcinoma. *Proteomics* **2006**, *6*, 2259-2272.

116. Unwin, R.D.; Craven, R.A.; Harnden, P.; Hanrahan, S.; Totty, N.; Knowles, M.; Eardley, I.; Selby, P.J.; Banks, R.E. Proteomic changes in renal cancer and co-ordinate demonstration of both the glycolytic and mitochondrial aspects of the Warburg effect. *Proteomics* **2003**, *3*, 1620-1632.

117. Ren, P.; Ye, H.; Dai, L.; Liu, M.; Liu, X.; Chai, Y.; Shao, Q.; Li, Y.; Lei, N.; Peng, B. Peroxiredoxin 1 is a tumor-associated antigen in esophageal squamous cell carcinoma. *Oncol. Rep.* **2013**, *30*, 2297-2303.

118. Anwar, S.; Yanai, T.; Sakai, H. Overexpression of Peroxiredoxin 6 Protects Neoplastic Cells against Apoptosis in Canine Haemangiosarcoma. *J. Comp. Pathol.* **2016**, *155*, 29-39, doi:https://doi.org/10.1016/j.jcpa.2016.05.002.

119. Yun, H.-M.; Park, K.-R.; Lee, H.P.; Lee, D.H.; Jo, M.; Shin, D.H.; Yoon, D.-Y.; Han, S.B.; Hong, J.T. PRDX6 promotes lung tumor progression via its GPx and iPLA2 activities. *Free Radic. Biol. Med.* **2014**, *69*, 367-376, doi:https://doi.org/10.1016/j.freeradbiomed.2014.02.001.

120. Sherbet, G.V.; Cajone, F. Stathmin in cell proliferation and cancer progression. *Cancer Genomics Proteomics* **2005**, *2*, 227-238.

121. Fang, L.; Min, L.; Lin, Y.; Ping, G.; Rui, W.; Ying, Z.; Xi, W.; Ting, H.; Li, L.; Ke, D. Downregulation of stathmin expression is mediated directly by Egr1 and associated with p53 activity in lung cancer cell line A549. *Cell. Signal.* **2010**, *22*, 166-173.

122. Kim, D.-W.; Kim, J.-Y.; Moon, J.H.; Kim, K.-B.; Kim, T.-S.; Hong, S.-J.; Cheon, Y.P.; Pak, J.H.; Seo, S.-B. Transcriptional induction of minichromosome maintenance protein 7 (Mcm7) in human cholangiocarcinoma cells treated with Clonorchis sinensis excretory–secretory products. *Mol. Biochem. Parasitol.* **2010**, *173*, 10-16, doi:http://dx.doi.org/10.1016/j.molbiopara.2010.03.005.

123. Luo, J.-H. Oncogenic activity of MCM7 transforming cluster. *World J. Clin. Oncol.* **2011**, *2*, 120.

124. Milton, R.H.; Abeti, R.; Averaimo, S.; DeBiasi, S.; Vitellaro, L.; Jiang, L.; Curmi, P.M.; Breit, S.N.; Duchen, M.R.; Mazzanti, M. CLIC1 function is required for β-amyloid-induced generation of reactive oxygen species by microglia. *The Journal of Neuroscience* **2008**, *28*, 11488-11499.

125. Barrès, V.; Ouellet, V.; Lafontaine, J.; Tonin, P.N.; Provencher, D.M.; Mes-Masson, A.-M. An essential role for Ran GTPase in epithelial ovarian cancer cell survival. *Mol. Cancer* **2010**, *9*, 1.

126. Caputo, E.; Wang, E.; Valentino, A.; Crispi, S.; De Giorgi, V.; Fico, A.; Ficili, B.; Capone, M.; Anniciello, A.; Cavalcanti, E. Ran signaling in melanoma: Implications for the development of alternative therapeutic strategies. *Cancer Lett.* **2015**, *357*, 286-296.

127. Zhao, J.; Meyerkord, C.L.; Du, Y.; Khuri, F.R.; Fu, H. 14-3-3 proteins as potential therapeutic targets. *Semin. Cell Dev. Biol.* **2011**, *22*, 705-712, doi:https://doi.org/10.1016/j.semcdb.2011.09.012.

128. Klemm, C.; Dommisch, H.; Göke, F.; Kreppel, M.; Jepsen, S.; Rolf, F.; Dommisch, K.; Perner, S.; Standop, J. Expression profiles for 14-3-3 zeta and CCL20 in pancreatic cancer and chronic pancreatitis. *Pathology-Research and Practice* **2014**, *210*, 335-341.

129. Chen, M.; Huang, H.; He, H.; Ying, W.; Liu, X.; Dai, Z.; Yin, J.; Mao, N.; Qian, X.; Pan, L. Quantitative proteomic analysis of mitochondria from human ovarian cancer cells and their paclitaxel-resistant sublines. *Cancer Sci.* **2015**, *106*, 1075-1083.

130. Niemantsverdriet, M.; Wagner, K.; Visser, M.; Backendorf, C. Cellular functions of 14-3-3ζ in apoptosis and cell adhesion emphasize its oncogenic character. *Oncogene* **2008**, *27*, 1315-1319.

131. Livinskaya, V.A.; Barlev, N.A.; Nikiforov, A.A. Immunoaffinity purification of the functional 20S proteasome from human cells via transient overexpression of specific proteasome subunits. *Protein Expr. Purif.* **2014**, *97*, 37-43.

132. Moghanibashi, M.; Jazii, F.R.; Soheili, Z.-S.; Zare, M.; Karkhane, A.; Parivar, K.; Mohamadynejad, P. Proteomics of a new esophageal cancer cell line established from Persian patient. *Gene* **2012**, *500*, 124-133.

133. Hu, X.-T.; Chen, W.; Wang, D.; Shi, Q.-L.; Zhang, F.-B.; Liao, Y.-Q.; Jin, M.; He, C. The proteasome subunit PSMA7 located on the 20q13 amplicon is overexpressed and associated with liver metastasis in colorectal cancer. *Oncol. Rep.* **2008**, *19*, 441-446.

134. Langdon, S.P. Cancer Cell Culture: Methods and Protocols. In *Methods Mol. Med.*, Illustrated edition ed.; Langdon, S.P., Ed. Humana Press Inc: 2004; pp 133-138.

135. Holford, J.; Beale, P.; Boxall, F.; Sharp, S.; Kelland, L. Mechanisms of drug resistance to the platinum complex ZD0473 in ovarian cancer cell lines. *Eur. J. Cancer* **2000**, *36*, 1984-1990.

136. Dhara, S. A rapid method for the synthesis of cis-[Pt (NH3) 2Cl2]. *Indian J. Chem.* **1970**, *8*, 193-194.

137. Mosmann, T. Rapid colorimetric assay for cellular growth and survival: application to proliferation and cytotoxicity assays. *J. Immunol. Methods* **1983**, *65*, 55-63.

138. Chou, T.-C. Theoretical basis, experimental design, and computerized simulation of synergism and antagonism in drug combination studies. *Pharmacol. Rev.* **2006**, *58*, 621-681.

139. GENOMED. Purifying gDNA from Mammalian Cells. Availabe online: http://manualzz.com/doc/7146492/cst-genomic-dna-purification-kits----tissues (accessed on 2 Jun).

140. Holford, J.; Sharp, S.; Murrer, B.; Abrams, M.; Kelland, L. In vitro circumvention of cisplatin resistance by the novel sterically hindered platinum complex AMD473. *Br. J. Cancer* **1998**, *77*, 366.

141. Maloney, A.; Clarke, P.A.; Naaby-Hansen, S.; Stein, R.; Koopman, J.-O.; Akpan, A.; Yang, A.; Zvelebil, M.; Cramer, R.; Stimson, L. Gene and protein expression profiling of human ovarian cancer cells treated with the heat shock protein 90 inhibitor 17-allylamino-17-demethoxygeldanamycin. *Cancer Res.* **2007**, *67*, 3239-3253.

142. Wood, R. Bio-Rad Protein Assay. Availabe online: http://www.bio-rad.com/webroot/web/pdf/lsr/literature/LIT33.pdf (accessed on 2 Jun).

143. Bradford, M.M. A rapid and sensitive method for the quantitation of microgram quantities of protein utilizing the principle of protein-dye binding. *Anal. Biochem.* **1976**, *72*, 248-254.

144. Bio-Rad. ReadyPrep 2-D Starter Kit. Availabe online: http://www.bio-rad.com/webroot/web/pdf/lsr/literature/4110009A.pdf (accessed on 2 Jun).

145. Bio-Rad. 2-D Electrophoresis Workflow How-To Guide. Availabe online: http://www.bio-rad.com/webroot/web/pdf/lsr/literature/Bulletin_2651.pdf (accessed on 2 Jun).

146. Bio-Rad. Criterion Dodeca Cell. Availabe online: http://www.bio-rad.com/webroot/web/pdf/lsr/literature/4006197a.pdf (accessed on 2Jun).

147. Bio-Rad. ChemiDoc XRS+Systems with Image Lab Software User Guid. Availabe online: http://www.bio-rad.com/webroot/web/pdf/lsr/literature/10017218.pdf (accessed on 2 Jun).

148. Bio-Rad. Melanie 3 User Manual. Availabe online: https://www.bio-rad.com/webroot/web/pdf/lsr/literature/4000151A.pdf (accessed on 2 Jun).

149. Winnik, W.M.; DeKroon, R.M.; Jeong, J.S.; Mocanu, M.; Robinette, J.B.; Osorio, C.; Dicheva, N.N.; Hamlett, E.; Alzate, O. Analysis of proteins using DIGE and MALDI mass spectrometry. In *Difference Gel Electrophoresis (DIGE) Methods and Protocols*, Humana Press: 2012; Vol. 854, pp. 47-66.